HHS Public Access

Author manuscript

Cell Rep. Author manuscript; available in PMC 2021 September 21.

Published in final edited form as:

Cell Rep. 2021 August 31; 36(9): 109626. doi:10.1016/j.celrep.2021.109626.

Mutant U2AF1-induced alternative splicing of *H2afy* (macroH2A1) regulates B-lymphopoiesis in mice

Sanghyun P. Kim[1], **Sridhar N. Srivatsan**[1], **Monique Chavez**[1], **Cara L. Shirai**[2], **Brian S. White**[1], **Tanzir Ahmed**[1], **Michael O. Alberti**[2], **Jin Shao**[1], **Ryan Nunley**[3], **Lynn S. White**[4], **Jeff Bednarski**[4], **John R. Pehrson**[5], **Matthew J. Walter**[1,6,*]

[1]Division of Oncology, Department of Internal Medicine, Washington University School of Medicine, St Louis, MO 63110, USA

[2]Department of Pathology and Immunology, Washington University School of Medicine, St Louis, MO 63110, USA

[3]Department of Orthopedic Surgery, Washington University School of Medicine, Barnes-Jewish Hospital, St. Louis, MO 63110, USA

[4]Department of Pediatrics, Washington University School of Medicine, St Louis, MO 63110, USA

[5]Department of Animal Biology, School of Veterinary Medicine, University of Pennsylvania, Philadelphia, PA 19104, USA

[6]Lead contact

SUMMARY

Somatic mutations in spliceosome genes are found in ~50% of patients with myelodysplastic syndromes (MDS), a myeloid malignancy associated with low blood counts. Expression of the mutant splicing factor U2AF1(S34F) alters hematopoiesis and mRNA splicing in mice. Our understanding of the functionally relevant alternatively spliced target genes that cause hematopoietic phenotypes *in vivo* remains incomplete. Here, we demonstrate that reduced expression of *H2afy1.1*, an alternatively spliced isoform of the histone H2A variant gene *H2afy*, is responsible for reduced B cells in U2AF1(S34F) mice. Deletion of *H2afy* or expression of U2AF1(S34F) reduces expression of *Ebf1* (early B cell factor 1), a key transcription factor for B cell development, and mechanistically, H2AFY is enriched at the EBF1 promoter. Induced expression of *H2AFY1.1* in U2AF1(S34F) cells rescues reduced EBF1 expression and B cells

*Correspondence: mjwalter@wustl.edu.

AUTHOR CONTRIBUTIONS

The study was designed by S.P.K. and M.J.W. Mouse characterization was done by S.P.K. and M.C., and data analysis was by S.P.K., M.J.W., M.O.A., L.S.W., J.B., and J.R.P. Nanostring design and data generation was performed by B.S.W., C.L.S., S.N.S., and M.J.W. RNA-seq was done by S.P.K. Bioinformatic analysis of data was performed by S.P.K., S.N.S., B.S.W., and M.J.W. S.P.K., J.S., R.N., and T.A. analyzed clinical samples. S.P.K. and M.J.W. wrote the paper.

DECLARATION OF INTERESTS

R.N. is a paid consult for Biocomposites, DePuy, Medical Compression Systems, Inc., Mirus, Cardinal Health, Halyard, Medtronic, and Smith & Nephew. R.N. receives research support from Biomet, Medical Compressions Systems, Stryker, DePuy, and Smith & Nephew. The other authors declare no competing interests.

SUPPLEMENTAL INFORMATION

Supplemental information can be found online at https://doi.org/10.1016/j.celrep.2021.109626.

numbers *in vivo*. Collectively, our data implicate alternative splicing of *H2AFY* as a contributor to lymphopenia induced by U2AF1(S34F) in mice and MDS.

Graphical Abstract

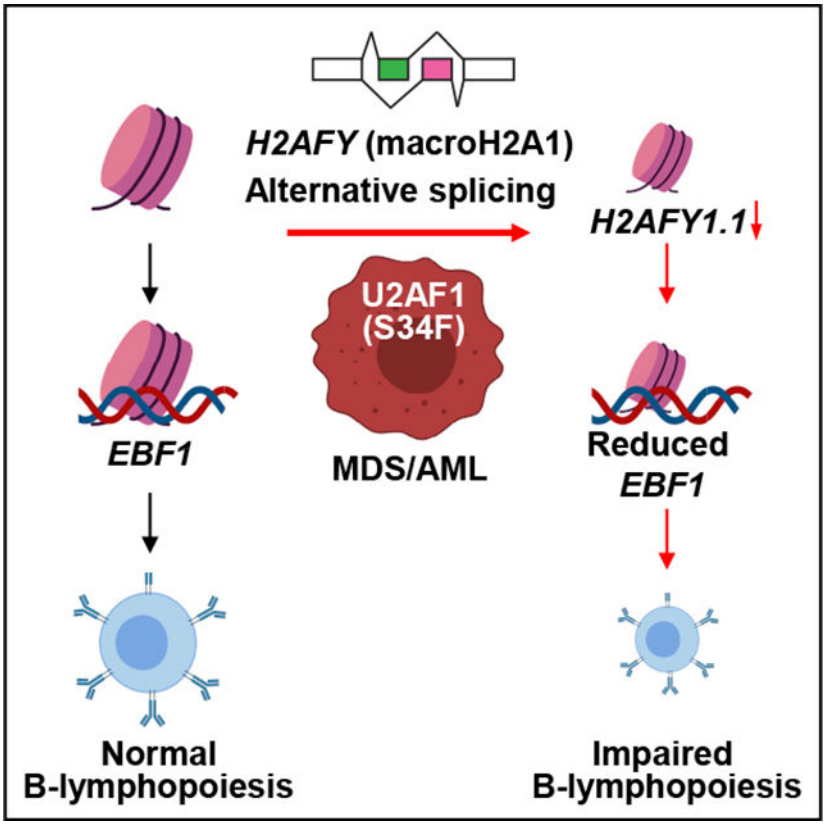

In brief

Kim et al. demonstrate that *H2AFY* is a functional target of U2AF1(S34F)-induced alternative splicing, a common spliceosome gene mutation in myelodysplastic syndromes. *H2afy*$^{-/-}$ and U2AF1(S34F) mice have similar defective B cell development. H2AFY occupies the *Ebf1* promoter, a key B cell differentiation transcription factor, providing a potential mechanism to regulate its expression.

INTRODUCTION

Myelodysplastic syndromes (MDS) are the most common myeloid cell malignancies in adults. MDS are a heterogenous group of clonal hematopoietic stem cell disorders characterized by ineffective hematopoiesis leading to low blood counts, including B lymphopenia, and dysplasia of one or more hematopoietic cell lineages. Sequencing studies have identified recurrent somatic mutations in spliceosome genes (most commonly in *SF3B1*, *SRSF2*, *U2AF1*, and *ZRSR2*) in over half of MDS patients (Damm et al., 2012; Graubert et al., 2011; Papaemmanuil et al., 2011; Thol et al., 2012; Visconte et al., 2012; Yoshida et al., 2011). Using genetically engineered mouse models, we and others have

reported that expression of common spliceosome gene mutants—including U2AF1(S34F), SRSF2(P95H), and SF3B1(K700E)—leads to alterations in RNA splicing and hematopoiesis in mice, including a reduction of mature hematopoietic cells, recapitulating features of human MDS (Fei et al., 2018; Kim et al., 2015b; Kon et al., 2018; Mupo et al., 2017; Obeng et al., 2016; Shirai et al., 2015; Smeets et al., 2018).

Whether alternative splicing of specific target RNAs by mutant splicing factors causes hematopoietic phenotypes and/or contributes to MDS pathogenesis is an active area of research. Splicing of *H2AFY*, *ATG7*, and *STRAP* (by U2AF1[S34F]) or *Ezh2* (by SRSF2[P95H]) was shown to be dysregulated in splicing factor mutant cells. Altering the splicing of these target genes can recapitulate or rescue the mutant-splicing-factor-induced phenotypes *in vitro* (Kim et al., 2015b; Park et al., 2016; Yip et al., 2017). However, it remains to be tested whether U2AF1 mutant-induced splicing changes directly contribute to altered hematopoiesis *in vivo* or are simply a biomarker of spliceosome gene mutations without functional significance.

H2AFY (also known as macroH2A1) is a histone H2A variant gene that has a role in metabolic functions, transcriptional gene regulation, and DNA damage response (Boulard et al., 2010; Changolkar and Pehrson, 2006; Changolkar et al., 2010; Gamble et al., 2010; Posavec Marjanović et al., 2017). *H2AFY* encodes two splice isoforms, *H2AFY1.1* and *H2AFY1.2* (also known as macroH2A1.1 and macroH2A1.2, respectively), and alternative splicing induced by U2AF1(S34F) expression leads to reductions in the *H2AFY1.1* isoform (Fei et al., 2018; Ilagan et al., 2015; Shirai et al., 2015; Yip et al., 2017). Reduced expression of *H2AFY1.1* has also been reported in a variety of solid tumors (Li et al., 2016; Novikov et al., 2011; Sporn and Jung, 2012; Sporn et al., 2009). In addition, Bereshchenko et al. (2019) recently reported that mice lacking H2AFY1.1 showed altered hematopoiesis, including increased myeloid cells and decreased B cells. However, whether reduced *H2afy1.1* expression is responsible for U2AF1(S34F)-induced hematopoietic phenotypes *in vivo* remains to be determined. In this study, we investigated whether alternative splicing of *H2AFY* contributes to hematopoietic phenotypes and MDS pathogenesis in patients expressing mutant U2AF1(S34F).

RESULTS

H2afy is a target gene of U2AF1(S34F)-induced alternative splicing

We previously reported that expression of U2AF1(S34F) results in hematopoietic phenotypes, including increased hematopoietic stem/progenitor cells, increased monocytes, and reduced B cells in mice (Shirai et al., 2015). We hypothesized that alternative splicing of specific target genes induced by U2AF1(S34F) directly contributed to hematopoietic phenotypes. To address the hypothesis, we analyzed three available RNA sequencing (RNA-seq) datasets that compared wild-type (WT) U2AF1 versus mutant U2AF1 samples (cultured human $CD34^+$ cells [Okeyo-Owuor et al., 2015], mouse common myeloid progenitors (CMPs) [Shirai et al., 2015], and human acute myeloid leukemia samples [Ley et al., 2013]) and identified 13 genes that showed similar alternative splicing across the three RNA-seq datasets (Shirai et al., 2015). We designed probes to interrogate isoform-specific expression for 8 of the 13 genes; 5 genes were not tested due to technical

difficulties. Nanostring analysis orthogonally validated alternative splicing of these target genes in mouse CMPs, monocytes, and B cells—the hematopoietic cell types that are altered by U2AF1(S34F) expression in mice (Figure 1A). Expression of all 8 isoforms was significantly altered in mouse CMPs (false discovery rate [FDR] < 0.1), with variable alterations in the monocytes and B cells. *H2afy* had consistent alternative splicing in all the three cell types, with greater than a 2-fold reduction in *H2afy1.1* isoform expression in U2AF1(S34F) mutant cells (Figure 1A). The two splice isoforms of *H2afy*—*H2afy1.1* and *H2afy1.2*—share all but exon 6 (mutually exclusive use of exon 6) (Figure 1B). Based on these lines of evidence, we hypothesized that alternative splicing of *H2AFY* contributed to the U2AF1(S34F)-induced hematopoietic phenotypes and MDS pathobiology. We addressed this hypothesis in three steps. First, we characterized *H2afy*$^{-/-}$ mice to delineate the role of *H2afy* in normal hematopoiesis. Second, we performed a complementation assay by re-expressing *H2AFY1.1* in *H2afy*$^{-/-}$ hematopoietic cells to identify *H2AFY1.1*-dependent hematopoietic phenotypes. Third, we determined whether *H2AFY1.1* expression can rescue altered hematopoiesis in U2AF1(S34F) mutant mice by re-expressing *H2AFY1.1* in U2AF1(S34F) hematopoietic cells.

H2afy knockout mice carry a constitutive deletion of exon 2 and lack expression of both *H2afy1.1* and *H2afy1.2* isoforms (Changolkar et al., 2007). *H2afy* knockout mice are viable, born at the expected Mendelian frequency, and have reduced or absent H2AFY protein expression in *H2afy*$^{+/-}$ and *H2afy*$^{-/-}$ bone marrow cells, respectively (Figure S1A). To study the hematopoietic-cell-intrinsic effect of *H2afy* loss in mice (including both *H2afy1.1* and *H2afy1.2* isoforms), we transplanted donor bone marrow cells from *H2afy*$^{+/+}$, *H2afy*$^{+/-}$, and *H2afy*$^{-/-}$ littermate mice into lethally irradiated congenic recipients (Figure 1C). At 4 months post-transplant, *H2afy*$^{-/-}$ recipients had reduced peripheral blood white blood cell counts (WBCs) (Figure 1D). In the peripheral blood, bone marrow, and spleen of recipient mice, we observed a reduction in *H2afy*$^{+/-}$ and *H2afy*$^{-/-}$ B cells in a gene dose-dependent manner, but normal monocytes and hematopoietic stem and progenitor numbers, including CMPs, in null mice (Figures 1E, 1F, S1B, and S1C). These data suggest that reduced expression of *H2afy1.1* contributes to lower mature B cell numbers but not to the CMP and monocyte phenotypes observed in U2AF1(S34F) mice. Next, we assessed the bone marrow B cell progenitor numbers in *H2afy*$^{+/+}$, *H2afy*$^{+/-}$, and *H2afy*$^{-/-}$ mice using a methylcellulose colony forming unit (CFU) assay (CFU-pre-B). Relative to *H2afy*$^{+/+}$ mice, *H2afy*$^{+/-}$ and *H2afy*$^{-/-}$ mice had reduced CFU-pre-B colony numbers (Figure 1G) but preserved myeloid CFUs (CFU-C; data not shown). Reduced CFU-pre-B numbers suggested a functional defect of B cell progenitors with *H2afy* loss. Next, we examined the stem/progenitor cell function of *H2afy*-deficient cells using a competitive repopulation assay.

H2afy$^{-/-}$ mice have defective B cell development in the bone marrow

We focused on comparing *H2afy*$^{-/-}$ hematopoietic cells to WT control cells because *H2afy*$^{-/-}$ hematopoietic cells are an ideal platform to perform complementation assays for re-expressing the individual *H2afy* splice isoforms to study their role in hematopoiesis. Test bone marrow cells (CD45.2^{+}) from *H2afy*$^{+/+}$ or *H2afy*$^{-/-}$ mice were mixed with an equal number of WT congenic competitor cells (CD45.1^{+}/45.2^{+}) and transplanted into lethally irradiated congenic recipient mice (CD45.1^{+}) (Figure 2A). The competitive repopulation

assays revealed a disadvantage for *H2afy*$^{-/-}$ stem/progenitor cells compared to *H2afy*$^{+/+}$ cells in primary recipient mice based on peripheral blood chimerism (Figure 2B). The competitive disadvantage of *H2afy*$^{-/-}$ donor cells was largely due to reductions in *H2afy*$^{-/-}$ B cells in the bone marrow, peripheral blood, and spleen of recipient mice (Figures 2C, S2A, and S2B). *H2afy*$^{-/-}$ bone marrow monocytes, neutrophils, and hematopoietic stem and progenitor cells also showed significant but modest reductions in recipient mice (Figures 2C and S2C). Given the significant reductions in *H2afy*$^{-/-}$ donor-cell-derived mature B cells, we examined B cell development in these mice. While B cell progenitors—including all-lymphoid progenitors (ALPs), B-cell-biased lymphoid progenitors (BLPs), and Hardy fraction A (also known as pre-pro B cells) (Hardy et al., 1991)—were no different between *H2afy*$^{+/+}$ and *H2afy*$^{-/-}$ cells, we observed marked reductions in all stages from *H2afy*$^{-/-}$ pro-B cells through mature B cells (Figure 2D). Next, we examined whether U2AF1(S34F) mice had similar B cell development defects that may be due to reduced *H2afy1.1* expression.

U2AF1(S34F) expression induces defective B cell development similar to *H2afy* loss

We examined whether the B cell developmental defects observed in *H2afy*-null mice occur in U2AF1(S34F) mice, which have reduced expression of the *H2afy1.1* isoform (Shirai et al., 2015). Because our previous study investigated the effect of U2AF1(S34F) expression in a mixed genetic background, we backcrossed the doxycycline-inducible U2AF1(WT) and U2AF1(S34F) transgenic mice to C57BL/6 mice at least 10 times (hereafter, we refer to these mice as U2AF1(WT) and U2AF1(S34F) mice, respectively). To explore the hematopoietic-cell-intrinsic effect of U2AF1(S34F) expression on B cell development, we transplanted bone marrow cells from U2AF1 (WT) or U2AF1(S34F) mice into lethally irradiated congenic recipients. Expression of U2AF1(S34F) led to significant reductions in WBCs, peripheral blood B cells, and bone marrow B cells in recipient mice compared to U2AF1(WT) expression (Figures 3A–3C). In addition, U2AF1(S34F) expression led to defective B cell development characterized by reduced pro-B through mature B cells (Figure 3D), similar to that observed in *H2afy*$^{-/-}$ mice. CFU-pre-B colony numbers were also reduced in U2AF1(S34F) compared to U2AF1(WT) recipients (Figure 3E), corroborating defective B cell development with U2AF1(S34F) expression. Collectively, the data demonstrate that U2AF1 (S34F) expression leads to defective B cell development similar to *H2afy* loss.

Ebf1 expression is reduced in *H2afy*$^{-/-}$ BLPs

Next, we investigated the mechanism underlying the defect in maturation from *H2afy*$^{-/-}$ pre-pro-B cells to pro-B cells—the first step of B cell differentiation defect upon *H2afy* loss. Because H2AFY is known to transcriptionally regulate target gene expression (Changolkar and Pehrson, 2006; Changolkar et al., 2010), we hypothesized that H2AFY transcriptionally regulates expression of a critical gene(s) involved in B cell development. To address this possibility, we performed RNA-seq on immunophenotypically defined bone marrow BLPs from *H2afy*$^{+/+}$ and *H2afy*$^{-/-}$ mice (Figures 4A and S4A). BLPs were selected because they are immediately upstream of the affected pro-B cells, and BLPs express high levels of *H2afy* RNA (RNA-seq data from the ImmGen consortium; Heng et al., 2008) (Figure S3). First, we confirmed the expected lack of *H2afy* exon 2 expression in *H2afy*$^{-/-}$ samples

(Figure 4B). Next, we identified 214 differentially expressed genes (DEGs) with FDR < 0.1 between *H2afy*$^{+/+}$ and *H2afy*$^{-/-}$ cells (Figure 4C; Table S1). The 214 DEGs segregated samples according to their genotypes, as expected (Figure 4C). Among the DEGs, we discovered that *early B cell factor 1* (*Ebf1*), a transcription factor critical for early B cell development, was downregulated in *H2afy*$^{-/-}$ BLPs (Figure 4D). In addition, downregulated DEGs were enriched in cell-cycle-and mitosis-associated pathways, and upregulated genes were involved in interferon signaling and the unfolded protein response (Table S2). We validated that the RNA and protein expression of *Ebf1* were reduced in *H2afy*$^{-/-}$ cells using qRT-PCR (Figure 4E) and intracellular flow cytometry (Figures 4F and S5A), respectively. In addition to reduced *Ebf1* expression, we found that known downstream targets of EBF1 were downregulated in *H2afy*$^{-/-}$ BLPs, including transcription factors (*Foxo1*, *Lef1*, *Id3*), and genes involved in V(D)J recombination (*Rag1*) and B cell functions (*Cd19*, *Vpreb2*, *Blnk*, etc.) (Figure 4D).

To examine the significance of reduced EBF1 expression upon *H2afy* loss, we compared the list of DEGs in *H2afy*$^{-/-}$ BLPs to known *Ebf1* targets genes identified in *Ebf1*$^{-/-}$ pre-pro-B cells (Jensen et al., 2018) and identified a significant overlap of 126 concordant DEGs between the two datasets (59%, $p < 0.001$), many with important functions for B cell development and/or function (Figure S4B; Table S3). Furthermore, the B cell phenotype of *H2afy*$^{-/-}$ mice (that have ~2-fold reduction in EBF1 levels) was similar to *Ebf1*$^{+/-}$ mice that have a reduction in pro-B through mature B cell stages, but not in ALPs or BLPs (Åhsberg et al., 2013). Collectively, the results suggested that reduced expression of *Ebf1* might be responsible for the defective B cell development of *H2afy*$^{-/-}$ B cell progenitors.

To study the mechanism whereby H2AFY regulates *Ebf1* expression, we examined the occupancy of H2AFY at the promoter of *Ebf1* by chromatin immunoprecipitation followed by qPCR, as previously described (Jiang et al., 2011). To measure occupancy of H2AFY at the *Ebf1* promoter in the context of early B cell development, we created WT and *H2afy*$^{-/-}$ pre-B cell lines by transforming *H2afy*$^{+/+}$ and *H2afy*$^{-/-}$ bone marrow cells with Abelson murine leukemia virus, respectively (Bredemeyer et al., 2006; Mainville et al., 2001). H2AFY enrichment at the *Ebf1* promoter, A-D regions, was significantly higher in the *H2afy*$^{+/+}$ compared to the *H2afy*$^{-/-}$ pre-B cell samples (Figure 4G). The data suggested that H2AFY was present at the promoter of *Ebf1* to regulate its expression. Taken together, the data demonstrated that *H2afy*$^{-/-}$ BLPs had reduced *Ebf1* and EBF1 target gene expression, suggesting that reduced *Ebf1* expression might contribute to the defective *H2afy*$^{-/-}$ B cell development.

Expression of *H2AFY1.1* in *H2afy*$^{-/-}$ bone marrow cells rescues reduced B cells *in vivo*

We next asked which *H2afy* isoform, *H2afy1.1* or *H2afy1.2*, was important for the defective B cell development as *H2afy*$^{-/-}$ mice lacked both isoforms. To address this question, we performed complementation assays by virally expressing either the *H2AFY1.1* or *H2AFY1.2* isoform in c-Kit-enriched *H2afy*$^{-/-}$ bone marrow cells, transplanting cells into lethally irradiated congenic recipients, and monitoring B cells (Figure 5A). Because human and mouse H2AFY are 98% identical at the amino acid level, and the exons specific to *H2afy1.1* or *1.2* isoforms are conserved, we expressed human *H2AFY1.1* or *H2AFY1.2*

in *H2afy*$^{-/-}$ mouse bone marrow cells. We first determined the effect of *H2AFY* isoform expression on B cell development by measuring the frequency of functional common lymphoid progenitors (CLPs) *ex vivo*. At 4 months post-transplant, GFP^{+} CLPs (i.e., transduced cells) were sorted at limiting dilutions in 96-well plates with an OP9 feeder layer and cultured for 1 week in the presence of mouse IL7 (interleukin 7). Expression of *H2AFY1.1* significantly increased the frequencies of functional CLPs that produced B cell progeny relative to control or *H2AFY1.2* expression, while expression of *H2AFY1.2* only modestly increased the frequencies of functional CLPs relative to control expression (Figure 5B). We next examined the *in vivo* effect of H2AFY1.1 or H2AFY1.2 expression in *H2afy*-null cells. Analysis of GFP^{+} cells in the peripheral blood (Figure 5C) and the bone marrow (Figure 5D) 4 months post-transplant showed a significant increase in B cells following *H2AFY1.1* expression. These complementation assay results suggested that the H2AFY1.1 isoform played a major and important role in B-lymphopoiesis *in vivo*.

Expression of *H2AFY1.1* in U2AF1(S34F) bone marrow cells rescues reduced B cells *in vivo*

Next, we asked whether exogenous *H2AFY1.1* expression could rescue the B cell phenotype associated with reduced *H2afy1.1* expression in U2AF1(S34F) mice. We expressed *H2AFY1.1* or *H2AFY1.2* in c-Kit-enriched U2AF1(S34F) bone marrow cells and transplanted them into lethally irradiated congenic recipients (Figure 6A). Following engraftment of transduced cells, we induced U2AF1(S34F) expression with doxycycline treatment. Flow cytometric analysis of the peripheral blood of control, H2AFY1.1, and H2AFY1.2 recipients before doxycycline treatment (i.e., before inducing U2AF1(S34F) expression) revealed no differences in hematopoietic lineage distribution of cells, including B cells (Figure S6A). We also verified physiologic expression of exogenously expressed H2AFY1.1 or H2AFY1.2 relative to endogenous H2AFY (Figure S6B). A decrease in peripheral blood B cells numbers induced by expression of U2AF1(S34F) was abrogated by H2AFY1.1 expression compared to control transduced cells (Figures 6B and S6A). Similarly, the number of CFU-pre-B colonies was also increased in *H2AFY1.1*-expressing bone marrow cells compared to control or *H2AFY1.2*-expressing bone marrow, indicating exogenous *H2AFY1.1* expression rescued B cell development in U2AF1 (S34F) bone marrow cells (Figure 6C).

Next, we assessed whether EBF1 expression was altered in U2AF1(S34F) B cells by intracellular flow cytometric analysis. U2AF1(S34F) expression reduced the number of B220^{low}EBF1^{+} B cells (Figure 6D), and expression of *H2AFY1.1* in U2AF1(S34F)-expressing cells ameliorated the reduction in EBF1^{+} B cells, relative to control samples (Figure 6E). Similar to U2AF1(S34F) mice, bone marrow samples from MDS patients with mutant U2AF1(S34F/Y) have reduced pro-B cells, pre-BI, pre-BII cells, and B cells and reduced EBF1 levels in CLPs compared to healthy donor samples (Figures S6C–S6E and S5B; Table S4). Collectively, the data suggested that reduced expression of *H2AFY1.1* by U2AF1(S34F) might drive B cell phenotypes via reduced EBF1 expression.

DISCUSSION

In this study, we demonstrate that alternative splicing of *H2afy* contributes to abnormal hematopoiesis induced by U2AF1 (S34F) expression *in vivo*. *H2afy* knockout mice and transgenic U2AF1(S34F) mice share defective B-lymphopoiesis that is associated with reduced levels of EBF1, a master transcription factor necessary for B cell development. Our data support that H2AFY is present at the *Ebf1* promoter to regulate its expression and its downstream targets, many of which are important for normal B cell development. Furthermore, B cell frequencies and EBF1 levels are reduced in MDS samples with U2AF1 (S34F) mutations compared to healthy controls. Re-expression of *H2AFY1.1* rescues the reduction in B cells in both *H2afy*$^{-/-}$ and U2AF1(S34F) murine bone marrow cells *in vivo*, validating that alternative splicing of *H2afy* by U2AF1(S34F) is a functionally significant splicing event that regulates B cell development. Collectively, our data implicate alternative splicing of *H2AFY* as a contributor to lymphopenia in U2AF1(S34F) mutant MDS patients.

Multiple mechanisms exist for how spliceosome gene mutations contribute to MDS disease pathogenesis. These include R-loop formation (Chen et al., 2018; Nguyen et al., 2017, 2018; Singh et al., 2020), alterations in the kinetics of splicing (Coulon et al., 2014), and alternative splicing (Kim et al., 2015b; Park et al., 2016; Yip et al., 2017). However, whether these mechanisms contribute to altered hematopoiesis *in vivo* is not known. Here, we provide evidence that alternative splicing induced by a mutant spliceosome gene directly contributes to abnormal blood counts *in vivo*, in addition to being a biomarker. Because our data show that *H2afy* alternative splicing accounts for defective B-lymphopoiesis in U2AF1(S34F) mice, other alternatively spliced targets may be responsible for the additional hematopoietic phenotypes observed in U2AF1(S34F) mice, including reduced monocytes and expanded CMPs. While reduction of *H2AFY1.1* in human hematopoietic cells has also been implicated in altered erythroid and granulocyte/monocyte differentiation *in vitro* (Yip et al., 2017), we did not observe alterations in the development of those cell types in *H2afy*$^{-/-}$ mice, suggesting that a compensation may occur in the constitutive knockout mouse model, or there are differences due to *in vitro* versus *in vivo* models, or a species difference. Recently, Bereshchenko et al. (2019) described an *H2afy1.1*-specific knockout model, where the authors observed an increase in the frequency of MAC1^{+} myeloid cells and a reduced frequency of B cells in *H2afy1.1* knockout mice. Because the absolute number of MAC1^{+} myeloid or B cells was not reported, it is unclear whether loss of *H2afy1.1* affects the distribution of hematopoietic lineages or the absolute number of affected lineage cells. Overall, these findings are consistent with our *in vivo H2afy*-null cell complementation assay results, suggesting that the H2AFY1.1 isoform is the major contributor to B-lymphopoiesis *in vivo*.

Isoform switching between *H2AFY* splice isoforms *H2AFY1.1* and *H2AFY1.2* has been appreciated in many cellular development and tumorigenesis processes (Dardenne et al., 2012; Dell'Orso et al., 2016; Hodge et al., 2018; Novikov et al., 2011; Pehrson et al., 1997; Posavec Marjanović et al., 2017; Sun and Bernstein, 2019); however, the functional significance and the underlying mechanism of the alternative splicing of *H2afy* have not been fully understood. In this study, we report alternative splicing of *H2AFY* as a downstream target of mutant U2AF1(S34F) that results in impaired B lymphopoiesis. Our

data further suggest that H2AFY occupancy at the promoter region of *Ebf1* may directly regulate its expression as a potential mechanism underlying B cell deficiencies observed in U2AF1(S34F) mice and MDS patients with a *U2AF1* mutation. H2AFY is generally considered a transcription repressor because it was found to predominantly localize in inactive X chromosome and heterochromatin (Buschbeck et al., 2009; Changolkar and Pehrson, 2006; Costanzi and Pehrson, 1998). However, our data show that loss of *H2afy* correlates with reduced *Ebf1* expression, similar to several studies that reported positive transcriptional regulation by H2AFY in a context-dependent manner (Changolkar and Pehrson, 2006; Chen et al., 2014; Gamble et al., 2010; Pehrson et al., 2014; Sun et al., 2018), including one report that showed reduced *Ebf1* expression in fetal liver cells lacking both macroH2A1 and macroH2A2 (i.e., *H2afy* and *H2afy2*, respectively) (Pehrson et al., 2014). Of the two isoforms of *H2afy*, expression of H2AFY1.1 in *H2afy*-null and U2AF1(S34F) mouse bone marrow cells consistently rescued reduced B cells. Taken together, our data identify a unique role of mutant U2AF1 and its alternative splicing target, *H2AFY*, in B cell development.

Reduced B cells and B cell precursors in MDS patients have been previously recognized in MDS (Liu et al., 2020; Ogata et al., 2006; Reis-Alves et al., 2015; Sternberg et al., 2005). However, our understanding of the genetic causes of reduced B cells and B cell precursors in MDS patients is incomplete. In line with our data implicating a role for *U2AF1* mutations in B cell abnormalities in MDS, *SF3B1* mutations were found to be present in pro-B cells from MDS patients, directly implicating splicing factor mutations in cell-intrinsic B cell alterations (Mortera-Blanco et al., 2017). Mice expressing mutant SRSF2 (Kim et al., 2015b) or SF3B1 (Obeng et al., 2016) also show B cell deficiencies, suggesting the possibility that B cell deficiencies are not limited to U2AF1-mutated MDS but occur broadly in the pathophysiology of spliceosome gene-mutated MDS. B cell deficiencies and/or defective B cell development may not directly affect myeloid disease progression of MDS but could contribute to increased infectious complications in MDS (Mortera-Blanco et al., 2017). Future studies could test whether modulating the expression of specific splice isoforms (e.g., *H2AFY1.1*) using antisense oligonucleotides could improve cytopenias and morbidities in preclinical models and ultimately in patients with MDS.

STAR⋆METHODS

Detailed methods are provided in the online version of this paper and include the following:

KEY RESOURCES TABLE

REAGENT or RESOURCE	SOURCE	IDENTIFIER
Antibodies		
CD34 FITC	Thermo Fisher Scientific	Cat# 11–0341–82; RRID:AB_465021
CD11b PE	Thermo Fisher Scientific	Cat# MA1–10082; RRID:AB_11154207
c-Kit APC-e780	Thermo Fisher Scientific	Cat# 47–1172–82; RRID:AB_1582226
c-Kit APC	Thermo Fisher Scientific	Cat# 17–1172–82; RRID:AB_469433

REAGENT or RESOURCE	SOURCE	IDENTIFIER
CD115 PE	Thermo Fisher Scientific	Cat# 12–1152–81; RRID:AB_465807
GR1 APC-e780	Thermo Fisher Scientific	Cat# 47–5931–82; RRID:AB_1518804
B220 PerCP-cy5.5	Thermo Fisher Scientific	Cat# 45–0452–82; RRID:AB_1107006
CD3e APC	Thermo Fisher Scientific	Cat# A18605; RRID:AB_2535395
FLT3 APC	Thermo Fisher Scientific	Cat# 17–1351–82; RRID:AB_10717261
SCA1 PerCP-cy5.5	Thermo Fisher Scientific	Cat# 45–5981–82; RRID:AB_914372
CD45.2 FITC	Thermo Fisher Scientific	Cat# 11–0454–85; RRID:AB_465062
CD16/32-unconjugated	Thermo Fisher Scientific	Cat# 14–0161–86; RRID:AB_467135
NK1.1 PerCP-cy5.5	Thermo Fisher Scientific	Cat# 45–5941–82; RRID:AB_914361
CD11c PerCP-cy5.5	Thermo Fisher Scientific	Cat# 45–0114–82; RRID:AB_925727
CD3e PerCP-cy5.5	Thermo Fisher Scientific	Cat# 45–0031–82; RRID:AB_2534299
IgD e450	Thermo Fisher Scientific	Cat# 48–5993–82; RRID:AB_1272202
Ter119 BV605	Biolegend	Cat# 116239; RRID:AB_2562447
CD16/32 BV421	Biolegend	Cat# 101332; RRID:AB_2650889
GR1 BV605	Biolegend	Cat# 108440; RRID:AB_2563311
B220 BV605	Biolegend	Cat# 103243; RRID:AB_11203907
CD3e BV605	Biolegend	Cat# 145–2C11; RRID:AB_2565842
SCA1 PE-Cy7	Biolegend	Cat# 108114; RRID:AB_493596
CD150 PE	Biolegend	Cat# 115904; RRID:AB_313683
CD48 PE-Cy7	Biolegend	Cat# 103423; RRID:AB_2075050
CD45.1 BV421	Biolegend	Cat# 110732; RRID:AB_2562563
CD45.2 BV421	Biolegend	Cat# 109832; RRID:AB_2565511
Streptavidin BV421	Biolegend	Cat# 405225
CD41 BV605	Biolegend	Cat# 133921, AB_2563933
IL7RA Biotin	Biolegend	Cat# 135006, AB_2126118
EBF1 PE	BD Biosciences	Cat# 565494; RRID:AB_2739263
IgM APC	Thermo Fisher Scientific	Cat# 17–5790–82; RRID:AB_469458
CD19 PE-Cy7	Thermo Fisher Scientific	Cat# 25–0193–81; RRID:AB_657664
Ly6D FITC	BD Biosciences	Cat# 561148; RRID:AB_10562197
CD43 BV510	BD Biosciences	Cat# 563206; RRID:AB_2738069
CD20 PerCP-Cy5.5	BD Biosciences	Cat# 560736; RRID:AB_1727451
CD38 PE-Cy7	Thermo Fisher Scientific	Cat# 25–0389–41; RRID:AB_1724065
CD34 BV421	BD Biosciences	Cat# 562577; RRID:AB_2687922
CD10 BV605	BD Biosciences	Cat# 562978; RRID:AB_2737929
CD19 APC	BD Biosciences	Cat# 555415; RRID:AB_398597
CD14 FITC	BD Biosciences	Cat# 555397; RRID:AB_395798
CD56 FITC	BD Biosciences	Cat# 562794; RRID:AB_2737799
CD3 FITC	Thermo Fisher Scientific	Cat# 11–0038–42; RRID:AB_2043831
Human BD Fc Block	BD Biosciences	Cat# 564219; RRID:AB_2728082
H2AFY (total)	Cell Signaling Technology	Cat# 8551; RRID:AB_2797647
Histone H3	Abcam	Cat# ab1791; RRID:AB_302613
Anti-rabbit IgG HRP	Cell Signaling Technology	Cat# 7074; RRID:AB_2099233

REAGENT or RESOURCE	SOURCE	IDENTIFIER
Anti-mouse IgG HRP	Cell Signaling Technology	Cat# 7076; RRID:AB_330924
H2AFY antibody	Abcam	Cat# ab37264; RRID:AB_883064
Normal Rabbit IgG	Millipore Sigma	Cat# 12–370; RRID:AB_145841
Biological samples		
Human MDS samples	This paper	Washington University
Human healthy donor bone marrow samples	This paper	Washington University
Chemicals, peptides, and recombinant proteins		
Penicillin-Streptomycin	Thermo Fisher Scientific	Cat# 15140122
Iscove's Modified Dulbecco's Medium	Thermo Fisher Scientific	Cat# 12440061
DMEM	Thermo Fisher Scientific	Cat# 11960077
RPMI 1640 Medium	Thermo Fisher Scientific	Cat# 11875085
GlutaMAX Supplement	Thermo Fisher Scientific	Cat# 35050061
MEM Non-Essential Amino Acids Solution	Thermo Fisher Scientific	Cat# 11140050
Sodium Pyruvate (100 mM)	Thermo Fisher Scientific	Cat# 11360070
HEPES (1 M)	Thermo Fisher Scientific	Cat# 15630080
2-Mercaptoethanol	Thermo Fisher Scientific	Cat# 21985023
Dulbecco's PBS	Thermo Fisher Scientific	Cat# 14190136
HBSS	Thermo Fisher Scientific	Cat# 14175079
0.5M EDTA, pH 8.0	Corning	Cat# 46–034-CI
Fetal Bovine Serum	VWR	Cat# 89510–194
L-glutamine	Thermo Fisher Scientific	Cat# 25030081
RetroNectin® Recombinant Human Fibronectin Fragment	Takara	Cat# T100A
SuperSignal West Pico PLUS Chemiluminescent Substrate	Thermo Fisher Scientific	Cat# 34580
SuperSignal West Femto Maximum Sensitivity Substrate	Thermo Fisher Scientific	Cat# 34095
Recombinant Murine Il7	Peprotech	Cat# 217–17
Recombinant Murine SCF	Peprotech	Cat# 250–03
Recombinant Murine TPO	Peprotech	Cat# 315–14
Recombinant Murine Il3	Peprotech	Cat# 213–13
Recombinant Murine FLT3 ligand	Peprotech	Cat# 250–31L
Bovine Serum Albumin solution	Millipore Sigma	Cat# A9576–50ML
Wright Giemsa Solution Fucillo	Millipore Sigma	Cat# 64571–75
StemPro-34 SFM	Thermo Fisher Scientific	Cat# 10639011
4–15% Mini-PROTEAN® TGX Precast Protein Gels	Biorad	Cat# 4561086
Precision Plus Protein Dual Color Standards	Biorad	Cat# 1610374
Hybond 0.45 PVDF	GE Healthcare	Cat# 10600023
625 ppm doxycycline chow	TestDiet	Custom ordered
doxycycline hyclate	Millipore Sigma	D9891–1G

REAGENT or RESOURCE	SOURCE	IDENTIFIER
Critical commercial assays		
MethoCult M3630	Stemcell Technology	Cat# 03630
BD Cytofix/Cytoperm	BD Biosciences	Cat# 554714
CD117 (c-Kit) MicroBeads	Miltenyi Biotec	Cat# 130–091–224
SuperScript IV First-Strand Synthesis System	Thermo Fisher Scientific	Cat# 18091050
NucleoSpin® RNA XS	MACHEREY-NAGEL	Cat# 740902.10
QIAquick PCR Purification Kit	QIAGEN	Cat# 28104
Protein A Dynabeads	Thermo Fisher Scientific	Cat# 10001D
RNA 6000 Nano Kit	Agilent	Cat# 5067–1511
SYBR Green PCR Master Mix	Thermo Fisher Scientific	Cat# 4309155
SMARTer Ultra Low RNA kit	Clontech	Cat# 634890
miRNeasy kit	QIAGEN	Cat# 217004
SYBR green PCR Master mix	Thermo Fisher Scientific	Cat# 4309155
Deposited data		
BLP-RNA-seq	This paper	GEO: GSE125118
Ebf1 knockout RNA-seq	Jensen et al., 2018	GEO: GSM2879293
B cell development RNA-seq	Heng et al., 2008	GEO: GSE109125
RNA-seq analysis code	This paper	Github; https://github.com/sridnona/H2afy_creports
Western blot	This paper	Mendeley Data, V1, https://doi.org/10.17632/7xvb8bx5ct.1
Experimental models: Cell lines		
293T	ATCC	Cat# CRL-3216
K562	ATCC	Cat# CCL-243
OP9	ATCC	Cat# CRL-2749
H2afy$^{+/+}$ pre-B Abelson cells	This paper	N/A
H2afy$^{-/-}$ pre-B Abelson cells	This paper	N/A
Experimental models: Organisms/strains		
Mouse: *H2afy*$^{-/-}$	Changolkar et al., 2007	N/A
U2AF1(S34F)	Shirai et al., 2015	N/A
Rosa26-RTTA	Shirai et al., 2015	N/A
CD45.1 NCI B6-Ly5.1/Cr	Charles River	Cat# 564
CD45.1/CD45.2	This paper	N/A
Oligonucleotides		
H2afy mouse genotype forward primer: TCTTTGCAAGGGTCAGACG	Changolkar et al., 2007	N/A
H2afy mouse genotype reverse primer 1: ACTGGAGACAGCGCATTACC	Changolkar et al., 2007	N/A
H2afy mouse genotype reverse primer 2: CAACATAACCACCATGATCTCG	Changolkar et al., 2007	N/A

REAGENT or RESOURCE	SOURCE	IDENTIFIER
Ebf1 qRT-PCR forward primer: ATGAAGAGGTTGGATTCTG	Yang et al., 2014	N/A
Ebf1 qRT-PCR reverse primer: GCAGTTATTGTGTGATTCCT	Yang et al., 2014	N/A
Gapdh RT-PCR forward primer: TGCACCACCAACTGCTTAG	Shirai et al., 2015	N/A
Gapdh RT-PCR reverse primer: GGATGCAGGGATGATGTTC	Shirai et al., 2015	N/A
Ebf1-ChIP-primer A-forward: GAGGCTCGCTGATTGAAAAC	Jiang et al., 2011	N/A
Ebf1-ChIP-primer B-forward: GGATCTATTTATTGTCTGGGACGA	Jiang et al., 2011	N/A
Ebf1-ChIP-primer C-forward: AAAGGCAATTCACCCAGATG	Jiang et al., 2011	N/A
Ebf1-ChIP-primer D-forward: GAGGATCCTGGTGGATCAGA	Jiang et al., 2011	N/A
Ebf1-ChIP-primer E-forward: ACTTCTGGAGAGTAGTGACCGAGT	Jiang et al., 2011	N/A
Ebf1-ChIP-primer F-forward: CGCTCCTTCCAGTTTAGACG	Jiang et al., 2011	N/A
Ebf1-ChIP-primer G-forward: AAAAACTTGCCTGGTTGTGG	Jiang et al., 2011	N/A
Ebf1-ChIP-primer A-reverse: AAAGGGCCTGTTTCCCTAAA	Jiang et al., 2011	N/A
Ebf1-ChIP-primer B-reverse: GAAAACTGAAGAAGAGGGTGACAG	Jiang et al., 2011	N/A
Ebf1-ChIP-primer C-reverse: GAGAAGGCAGTGATGGTGGT	Jiang et al., 2011	N/A
Ebf1-ChIP-primer D-reverse: GTGGGTGGGTGTATTCCAAG	Jiang et al., 2011	N/A
Ebf1-ChIP-primer E-reverse: ATACGACTTTAGTAGACCGCAAGG	Jiang et al., 2011	N/A
Ebf1-ChIP-primer F-reverse: GTCATCCTTCCGCCTTATCA	Jiang et al., 2011	N/A
Ebf1-ChIP-primer G-reverse: GGGCTGGAGTTTCCTTTTGT	Jiang et al., 2011	N/A
Recombinant DNA		
H2AFY1.1 cDNA	Chadwick and Willard, 2001	Addgene 45166
H2AFY1.2 cDNA	Chadwick and Willard, 2001	Addgene 45168
Lenti-MND-IRES-GFP-Flag	Okeyo-Owuor et al., 2015	N/A
pMD-G	Okeyo-Owuor et al., 2015	N/A
pMD-Lg	Okeyo-Owuor et al., 2015	N/A
REV	Okeyo-Owuor et al., 2015	N/A
Software and algorithms		
nSolver Analysis Software	Nanostring	https://www.nanostring.com/products/analysis-solutions/ncounter-analysis-solutions/nsolver-data-analysis-support/
HISAT2 v.2.0.6	Kim et al., 2015a	http://daehwankimlab.github.io/hisat2/

REAGENT or RESOURCE	SOURCE	IDENTIFIER
HTseq v.0.11.0	Anders et al., 2015	https://htseq.readthedocs.io/en/release_0.11.0/
Voom	Law et al., 2014	https://www.rdocumentation.org/packages/limma/versions/3.28.14/topics/voom
EdgeR	Robinson et al., 2010	https://bioconductor.org/packages/release/bioc/html/edgeR.html
DESeq2	Love et al., 2014	https://bioconductor.org/packages/release/bioc/html/DESeq2.html
ELDA	Hu and Smyth, 2009	http://bioinf.wehi.edu.au/software/elda/
FastQC	The Babraham Institute	https://www.bioinformatics.babraham.ac.uk/projects/fastqc
STAR	Dobin et al., 2013	https://github.com/alexdobin/STAR
StringTie v.1.3.3	Pertea et al., 2015	https://github.com/gpertea/stringtie
Flowjo v.10.6	Treestar	RRID:SCR_008520
VarSCAn	Koboldt et al., 2012	http://varscan.sourceforge.net/

RESOURCE AVAILABILITY

Lead contact—Further information and requests for resources and reagents should be directed to and will be fulfilled by the Lead Contact, Matthew J. Walter (mjwalter@wustl.edu).

Materials availability—Abelson-transformed pre-B cells (*H2afy*$^{-/-}$ and *H2afy*$^{+/+}$) are available upon request.

Data and code availability

- RNA-seq data have been deposited at GEO and are publicly available as of the date of publication. Accession numbers are listed in the Key resources table. Original western blot images have been deposited at Mendeley and are publicly available as of the date of publication. The DOI is listed in the Key resources table.
- This paper analyzes existing, publicly available data. These accession numbers for the datasets are listed in the Key resources table.
- All original code has been deposited at GitHub and is publicly available as of the date of publication. DOIs are listed in the Key resources table.
- Any additional information required to reanalyze the data reported in this paper is available from the lead contact upon request.

EXPERIMENTAL MODEL AND SUBJECT DETAILS

Animal models—All mouse procedures were performed according to protocols approved by Institutional Animal Care and Use Committee at Washington University in St. Louis. *H2afy* knock-out mice were generated and described previously by Pehrson and colleagues (Changolkar et al., 2007). Transgenic U2AF1(WT) and U2AF1(S34F) mice were described

previously (Shirai et al., 2015). Transgenic U2AF1(WT) or U2AF1(S34F) mice were crossed with Rosa26-rtTA mice, and double transgenic mice with a single copy of a *U2AF1* transgene and an *rtTA* transgene were used for all experiments. Transgenic mouse colonies were maintained by breeding heterozygous, double transgenic [U2AF1(WT)/rtTA or U2AF1(S34F)/rtTA] mice to wild-type C57BL/6 mice. Doxycycline was administered via doxycycline-containing rodent chow (625 ppm doxycycline, pico 5053 base, TestDiet). All of the mice used in the experiments were backcrossed into the C57BL/6 background at least 10 times. For all experiments, wild-type littermate controls were used.

Human MDS samples and healthy donor bone marrow samples—The use of human MDS samples and healthy donor bone marrow samples was approved by the Washington University School of Medicine Institutional Review Board and with patients' consent for sample use. Studies were performed in accordance with the Declaration of Helsinki. Bone marrow cells were frozen and thawed for experiments. Clinical and genetic information for patient samples is included in Table S4.

Mouse bone marrow transplant and competitive repopulation assays—Bone Marrow Transplant of *H2afy*$^{+/+}$, *H2afy*$^{+/-}$ or *H2afy*$^{-/-}$ Cells

To generate mice for each experiment, one million whole bone marrow cells from three *H2afy*$^{+/+}$, *H2afy*$^{+/-}$ or *H2afy*$^{-/-}$ female mice were pooled (CD45.2) and transplanted into at least five lethally irradiated (1,100 rads, cesium-137 irradiator) wild-type congenic female recipient mice (CD45.1, NCI B6-Ly5.1/Cr, Charles River). Donor mice were between 8 and 12 weeks of age, and recipients were 7–12 weeks of age. Competitive repopulation assays were performed by mixing "test" whole bone marrow cells from three *H2afy*$^{+/+}$ or *H2afy*$^{-/-}$ female mice pooled (CD45.2) in equal proportions with "competitor" whole bone marrow cells from three female wild-type congenic mice (CD45.1/45.2, C57BL/6) pooled, and transplant of two million mixed cells into lethally irradiated (1,100 rads, cesium-137 irradiator) wild-type congenic female recipient mice (CD45.1, C57BL/6). Donor mice were between 6 and 12 weeks of age, and recipients were 7–12 weeks of age. Male donor and recipient mice were used for empty-vector, *H2AFY1.1*, and *H2AFY1.2* expression experiments.

Transplant of U2AF1(WT) and U2AF1(S34F) mouse bone marrow—To generate mice for experiments, one million whole bone marrow cells from three female U2AF1(WT)/rtTA or U2AF1(S34F)/rtTA pooled (CD45.2) were transplanted into ten lethally irradiated (1,100 rads, cesium-137 irradiator) wild-type congenic recipient female mice (CD45.1, NCI B6-Ly5.1/Cr, Charles River). Donor mice were between 8 and 12 weeks of age and recipients were 7–12 weeks of age. Male donor and recipient mice were used for empty-vector, *H2AFY1.1*, and *H2AFY1.2* expression experiments.

METHOD DETAILS

Cell staining and flow cytometry—Red blood cells of peripheral blood, bone marrow, or spleen were lysed by 5 minutes incubation in the ACK lysis buffer on ice. Cells were

treated with anti-mouse CD16/32 or human Fc block (BD Biosciences, Cat# 564219) and stained with the indicated combinations of the following antibodies:

Mouse mature lineage cell distribution—CD11b PE (clone M1/70), CD115 PE (clone AFS98), Gr-1 APC-e780 or BV605 (clone RB6–8C5), B220 PerCP-cy5.5 or BV605 (clone RA3–6B2), CD3 APC or BV605 (clone 145–2C11), CD45.1 BV421 (clone A20), and CD45.2 FITC or BV421 (clone 104).

Mouse stem and progenitor cells—Lineage-BV605 (Lin): $B220^+$, $CD3e^+$, $Gr\text{-}1^+$, $Ter\text{-}119^+$, or $CD41^+$; KLS: Lin^-, $Sca\text{-}1^+$, $c\text{-}Kit^+$; KLS-SLAM: Lin^-, $SCA\text{-}1^+$, $c\text{-}Kit^+$, $CD150^+$, $CD48^-$; GMP: Lin^-, $SCA\text{-}1^+$, $c\text{-}Kit^+$, $CD34^+$, $CD16/32^+$; CMP: Lin^-, $SCA\text{-}1^-$, $c\text{-}Kit^+$, $CD34^+$, $CD16/32^-$; MEP: Lin^-, $SCA\text{-}1^-$, $c\text{-}Kit^+$, $CD34^-$, $CD16/32^-$; CLP: Lin^-, $SCA\text{-}1^+$, $c\text{-}Kit^+$, $FLT3^+$, $IL7R\alpha^+$; ALP: Lin^-, $SCA\text{-}1^+$, $c\text{-}Kit^+$, $FLT3^+$, $IL7R\alpha^+$, $Ly6D^-$; BLP: Lin^-, $SCA\text{-}1^+$, $c\text{-}Kit^+$, $FLT3^+$, $IL7R\alpha^+$, $Ly6D^+$; Hardy Fraction A: $B220^+$, $NK1.1^-$, $CD3e^-$, $CD11c^-$, IgM^-, IgD^-, $CD19^-$, $Ly6D^+$; Hardy Fractions B-C: $B220^+$, $NK1.1^-$, $CD3e^-$, $CD11c^-$, IgM^-, IgD^-, $CD19^+$, $CD43^+$; Hardy Fractions D: $B220^+$, $NK1.1^-$, $CD3e^-$, $CD11c^-$, IgM^-, IgD^-, $CD19^+$, $CD43^-$; Hardy Fractions E: $B220^+$, $NK1.1^-$, $CD3e^-$, $CD11c^-$, IgM^+, IgD^-; Hardy Fractions F: $B220^+$, $NK1.1^-$, $CD3e^-$, $CD11c^-$, IgM^+, IgD^+.

Human B cells—$CD19^+$ B cells: $CD3^-$, $CD14^-$, $CD56^-$, $CD19^+$; CLP: $CD3^-$, $CD14^-$, $CD56^-$, $CD19^+$, CD19−, $CD20^-$, $CD34^+$, $CD10^+$; Pro-B: $CD3^-$, $CD14^-$, $CD56^-$, $CD19^+$, CD34+; Pre-BI: $CD3^-$, $CD14^-$, $CD56^-$, $CD19^+$, $CD38^+$, $CD34^-$; Pre-BII: $CD3^-$, $CD14^-$, $CD56^-$, $CD19^+$, $CD20^+$ Analysis was performed using a Gallios (Beckman Coulter) and data were analyzed using FlowJo version 10.4.2 (Treestar).

Intracellular mouse and human EBF1 protein staining for flow cytometry—Cells were stained for cell surface markers as described above and then fixed and permeabilized using the Cytofix/Cytoperm and the Permeabilization Buffer Plus kit (BD Pharmingen), respectively, according to the manufacturer's instructions. Intracellular EBF1 was stained with primary mouse EBF1 antibody conjugated with PE (1:100 dilution, Clone T26–818, BD Pharmingen) for 20 minutes at 4°C and analyzed by flow cytometry. The mean fluorescence intensity was calculated for the PE signal. Human and mouse EBF1 proteins are 100% homologous at the amino acid level, and we determined the cross-reactivity of the anti-mouse EBF1 antibody against human EBF1 using EBF1-negative 293T cells transiently transfected with human EBF1 expression plasmid.

Western blotting of H2AFY—Histone extracts were prepared using EpiQuik Total Histone Extraction Kit (EpiGentek) according to the manufacturer's instructions. Proteins were separated by SDS-PAGE using Mini-PROTEAN gels (4%–15%, Biorad) and transferred to PVDF membranes (EMD Millipore) at 20V overnight at 4°C. Membranes were incubated in 5% nonfat dry milk in Tris-buffered saline with 0.1% Tween-20 ((TBST) for 1 hour at room temperature and were probed with primary antibodies (H2AFY: reacting to both human and mouse, Cell Signaling Technology #8551; histone H3: Abcam ab1791) in 3% nonfat dry milk TBST for 2 hours at room temperature (Histone H3) or 16 hours at 4°C (H2AFY). Membranes were rinsed 4 times in TBST for 5 minutes and then incubated with horseradish-peroxidase–conjugated anti-rabbit (1:10000; Cell Signaling Technology #7074)

or anti-mouse (1:10000; Cell Signaling Technology #7076) secondary antibodies for 1 hour at room temperature. Membranes were then washed 4 times in TBST for 5 minutes each time, and ECL (SuperSignal West Pico PLUS, Thermo Fisher) was applied for 1 minute. Membranes were imaged with a myECL Imager (Thermo Fisher).

Colony forming assays—Bone marrow cells were harvested and lysed to remove red cells. One hundred thousand whole bone marrow cells or two hundred thousand bone marrow cells sorted for GFP were seeded in methylcellulose media (M3630, Stem Cell Technologies) to detect CFU-Pre-B per the manufacturer's instructions. To induce transgenic U2AF1(WT) or U2AF1(S34F) expression, doxycycline hyclate (75ng/mL, Millipore Sigma) in water was added to the media before cell seeding. CFU-Pre-B colonies were counted on days 7–8.

Nanostring assay and analysis—Samples for NanoString were generated similar to experiments previously described for transgenic U2AF1(S34F) and U2AF1(WT) mouse experiments (Shirai et al., 2015). Transgenic mouse donor cells (CD45.2, 1×10^6 cells from 2–3 mice pooled) from a mixed C57BL/6 3 129S4Sv/Jae strain (Shirai et al., 2015) were transplanted into lethally irradiated wild-type F1 (C57BL/6 3 129S4Sv/Jae) recipient mice (CD45.1/CD45.2). Following at least 6 weeks of bone marrow engraftment, transgene induction was performed *in vivo* for 5 days with 625 ppm doxycycline chow. U2AF1(S34F)- or U2AF1(WT)-expressing lineage specific cells were FACS sorted from bone marrow using a congenic marker (CD45.2) and the staining schemes as described above. RNA was extracted from sorted cells using the miRNeasy kit (QIAGEN), and a custom-designed Nanostring assay was performed using 100 ng of bulk RNA per the manufacturer's protocol (Nanostring Technologies). The Nanostring probesets were designed to query previously identified splice junctions perturbed by U2AF1(S34F) expression in mice, as defined by RNA-seq (Shirai et al., 2015). For each splice junction, a reporter/capture probe pair was constructed in such a way that the two probes targeted (were complementary to) the two exons on either side of the splice junction.

RCC files from Digital Analyzer were processed using nSolver Analysis Software (Nanostring) and custom R scripts to extract raw counts for downstream analysis. Log2 fold change for each probe was calculated by processing the raw counts using Voom (Law et al., 2014) followed by EdgeR (Robinson et al., 2010).

Limiting dilution assay for assessing functional CLP frequencies—One thousand OP9 cells were seeded onto 96 well plates a day before CLP sorting. On the next day, bone marrow cells were harvested and enriched for c-Kit$^+$ cells using CD117 MicroBeads on the autoMACS Pro Separator (Miltenyi Biotec). Subsequently, cells were stained, as described above, and 1, 4, 16, or 32 cells of GFP$^+$ CLPs were isolated (Moflo plate sorter, Beckman Coulter) directly into 96 well plates with OP9 feeder cells in RPMI1640 media containing 1% glutamine (GIBCO), 1% MEM non-essentail amino acids (GIBCO), 1% sodium pyruvate (GIBCO), 1% HEPES (GIBCO), 55 μM β-mercaptoethanol (GIBCO), 20 ng/mL SCF (Peprotech), 20 ng/mL FLT3 ligand (Peprotech), and 20 ng/mL IL7 (Peprotech). All of the growth factors were murine recombinant proteins. At day 3, media was replenished and at day 7, CD19$^+$ B cells were counted by flow cytometry

using a plate reader on the ZE5TM Cell Analyzer (Bio-rad). Limiting dilution analysis was performed using the ELDA program (http://bioinf.wehi.edu.au/software/elda/) (Hu and Smyth, 2009).

Cloning of H2AFY1.1 and H2AFY1.2 expression lentivirus plasmids and virus generation—cDNA sequences of *H2AFY1.1* and *1.2* were obtained from Addgene [H2AFY1.1 #45166, H2AFY1.2 # 45168, (Chadwick and Willard, 2001)] and were cloned into a lenti-MND-IRES-GFP-Flag vector as described previously (Okeyo-Owuor et al., 2015). Lentivirus was generated in 293T cells (ATCC, CRL-3216) with the packaging plasmids pMD-G, pMD-Lg and REV. Virus was tittered using K562 cells (ATCC, CCL243).

H2AFY1.1/H2AFY1.2 complementation assay—*H2AFY1.1* or *H2AFY1.2* was re-expressed either in *H2afy* null or in U2AF1(S34F) hematopoietic cells. A day before transduction, a 24-well untreated plate was coated with Retronectin (T100B, Clontech) per the manufacturer's instructions overnight at 4°C. Whole bone marrow cells from *H2afy* null or U2AF1(S34F) mice were c-Kit enriched using CD117 MicroBeads on the autoMACS Pro Separator (Miltenyi Biotec). Cells were then transferred to a Retronectin-coated plate and control lentivirus or *H2AFY1.1* or *1.2* expression lentivirus (MOI of 5) was added. Cells were spun at 1250G at 35°C for 90 minutes. Cells were rested in an incubator for 2 hours and warm media was added. The next day, 150,000 to 200,000 cells (CD45.2) were transplanted into lethally irradiated wild-type congenic recipients (CD45.1) via retro-orbital injection. Recipients of *H2afy* null bone marrow cells complemented with control, H2AFY1.1 or 1.2 were bled at each month to monitor GFP^+ lineage cell frequencies. At 4 months post-transplant, GFP^+ CLPs were sorted for a limiting dilution assay as outlined above. U2AF1(S34F)-recipients were bled at 4 weeks post-transplant to monitor chimerism, and treated with 625ppm doxycycline chow for 6 months when the mice were sacrificed for bone marrow analysis.

BLP RNA collection, library preparation, and sequencing—Bone marrow cells were harvested from $H2afy^{+/+}$ and $H2afy^{-/-}$ mice of 5–12 weeks of age. Cells were enriched for c-Kit^+ cells using CD117 MicroBeads on the autoMACS Pro Separator (Miltenyi Biotec). Subsequently, cells were stained according to the staining scheme described above, and BLPs were sorted by FACS (Moflo, Beckman Coulter) directly into the lysis buffer of NucleoSpin RNA XS kit (MACHEREY-NAGEL). RNA was isolated per manufacturer's instructions. Per sample, RNA equivalent of 5,000–15,000 BLPs from 2–3 mice were pooled. Total RNA integrity and concentration were assessed using a 2100 Bioanalyzer and an RNA 6000 Pico kit (Agilent). Library preparation was performed with 10–50ng of total RNA with a Bioanalyzer RIN score greater than 8.0. Double stranded-cDNA was prepared using the SMARTer Ultra Low RNA kit for Illumina Sequencing (Takara-Clontech) per manufacturer's protocol. cDNA was fragmented using a Covaris E220 sonicator using duty cycle 10, intensity 5, cycles/burst 200, time 180 s. cDNA was blunt ended, had an A base added to the 3′ ends, and then had Illumina sequencing adapters ligated to the ends. Ligated fragments were then amplified for 12 cycles using primers incorporating unique index tags. Fragments were sequenced on an Illumina HiSeq-3000 using single reads extending 50 bases.

RNA-seq analyses

BLPs RNA-seq: Read quality was assessed using FastQC (https://www.bioinformatics.babraham.ac.uk/projects/fastqc). Reads were mapped using HISAT2 (version 2.0.6) (Kim et al., 2015a) against the mm9 version of the mouse genome from Ensembl consortium. Reads were further processed using HTseq (version 0.11.0) (Anders et al., 2015). Differentially expressed genes were identified using DESeq2 (Love et al., 2014), following filtering out genes with fewer than 5 reads in the half of the samples. Differentially expressed genes were filtered using a false discovery rate (FDR) cutoff of < 10%. TPM values were calculated using StringTie (version 1.3.3) (Pertea et al., 2015). Gene enrichment analysis (GO ontology) was performed using Clusterprofiler (version 3.10.1) (Yu et al., 2012) against GO processes (e.g., Cellular-Components [CC], MF Molecular Function [MF], and Biological Process [BP]). Pathway enrichment analysis was performed using fgsea (version 1.8.0 [https://www.biorxiv.org/content/10.1101/060012v1]) and the pre-ranked function against GO, Reactome, and MSIGDB gene sets.

Ebf1 *knock-out pro-B cell RNA-seq*: The data were previously reported (Jensen et al., 2018). Raw reads were processed and analyzed by the same method as the above BLP RNA-seq dataset.

H2afy *RNA expression during B cell development*: Raw reads were downloaded from (https://www.ncbi.nlm.nih.gov/geo/query/acc.cgi?acc=GSE92434). Data are assembled by the ImmGen consortium (Heng et al., 2008). Read quality was assessed using FastQC and aligned against the mouse genome (mm9) using STAR (Dobin et al., 2013) as specified in the ImmGen protocols (https://www.immgen.org/Protocols/ImmGenULI_RNAseq_methods.pdf). Expression (TPM) of *H2afy* was calculated using StringTie (version 1.3.3) (Pertea et al., 2015).

***Ebf1* qRT-PCR:** BLP cells were sorted and RNA was isolated and quantified as described above. Two mice were pooled for each sample. RNA was converted to cDNA using SuperScript IV First-Strand Synthesis System (18091050, Thermo Fisher). *Ebf1* qRT-PCR [Ebf1 forward primer 5′-ATGAAGAGGTTGGATTCTG-3′, reverse primer 5′-GCAGTTATTGTGTGATTCCT-3′, primer sequences are from (Yang et al., 2014) and *Gapdh* qRT-PCR (Forward primer 5′-TGCACCACCAACTGCTTAG-3′, Reverse primer 5′-GGATGCAGGGAT GATGTTC-3′) were performed using the SYBR Green PCR Master Mix (4309155, Thermo Fisher) on StepOnePlus (Thermo Fisher). Individual cDNA samples were normalized to their levels of *Gapdh* using the delta delta Ct method.

Abelson transformed pre-B cells and H2AFY ChIP-qPCR—Viral (v)-Abl kinase-transformed pre-B cell lines were generated from *H2afy*$^{+/+}$ and *H2afy*$^{-/-}$ bone marrow cells. Bone marrow cells from these mice were cultured with the pMSCV-v-abl retrovirus to generate stable v-abl transformed pre-B cell lines, as described previously (Bredemeyer et al., 2006; Mainville et al., 2001). Abelson cells were cultured in DMEM (Cat# 11960077, Thermo Fisher) media supplemented with 10% FBS, 1% penicillin-streptomycin (Cat# 15140122, Thermo Fisher), 1% sodium pyruvate (Cat# 11360070, Thermo Fisher), 1% non-essential amino acids (Cat# 11140050, Thermo Fisher), 1% L-glutamine (Cat# 25030081,

Thermo Fisher) and 0.22 μM 2-mercaptoethanol (Cat# 21985023, Thermo Fisher). Cells were passaged every 2 days and maintained at less than 80% confluence.

ChIP was performed as previously described (Soodgupta et al., 2019). Briefly, 10 million cells in single-cell suspension was were crosslinked with 1% formaldehyde. Chromatin was isolated and digested by shearing with sonication, and immunoprecipitation was performed with anti-H2AFY antibody (Cat# ab37264, Abcam) or normal Rabbit IgG (12–370, Millipore Sigma) and Protein A Dynabeads (Cat# 10001D, Thermo Fisher). Immunoprecipitated DNA was then washed and eluted. Sheared input material and eluted DNA were purified with QIAquick PCR purification kit (Cat# 28104, QIAGEN). Purified DNA was amplified by RT-PCR using SybrGreen (Cat# 4309155, Thermo Fisher) on a StepOnePlus Real-Time PCR system (Thermo Fisher) and analyzed using the relative standard curve delta delta CT method as described previously (Jiang et al., 2011). The primers against the mouse *Ebf1* promoters are listed in Key resources table.

QUANTIFICATION AND STATISTICAL ANALYSIS

Details of statistical tests are indicated in the Figure Legends. Statistical analyses were performed using GraphPad Prism v7.00. Significance is indicated using the following convention: *p < 0.05, **p < 0.01, ***p < 0.001. Error bars on graphs represent the standard deviation of the mean.

Supplementary Material

Refer to Web version on PubMed Central for supplementary material.

ACKNOWLEDGMENTS

The authors thank Drs. Timothy Ley and Dan Link for helpful scientific discussions and Drs. Li Ding and Reyka Jayasinghe for discussion of *H2AFY* expression in various datasets. The authors thank Drs. Matthew Ndonwi, Shawn Jin, Tianjiao Wang, Sara Arenas, and Christian Rosa-Birriel for technical assistance. Dr. Kim Trinkaus at the Siteman Cancer Center Biostatistics Shared Resource provided helpful advice regarding the limiting dilution assay. This work was supported by the Siteman Cancer Center (Cancer Biology Pathway pre-doctoral fellowship T32 CA113275 and P30 CA091842 to S.P.K.) and grants from the Edward P. Evans Foundation (to M.J.W.), the Taub Foundation (to M.J.W.), the Lottie Caroline Hardy Trust (to M.J.W.), an NIH/NCI grant (K12 CA167540; to B.S.W., M.O.A., and C.L.S.), and a Clinical and Translational Award from the NIH National Center for Advancing Translational Sciences (UL1 TR000448 to B.S.W.). Support for procurement of human samples and research was provided by the Genomics of AML Program Project of the NCI (P01 CA101937) and the Specialized Program of Research Excellence in AML (P50 CA171963). Core services were provided by the Siteman Cancer Center Tissue Procurement Core, the Flow Cytometry Core, the Genome Technology Access Center, and the Division of Comparative Medicine at Washington University School of Medicine. The Siteman Cancer Center is supported in part by NCI Cancer Center Support grant P30 CA091842.

REFERENCES

Åhsberg J, Ungerbäck J, Strid T, Welinder E, Stjernberg J, Larsson M, Qian H, and Sigvardsson M (2013). Early B-cell factor 1 regulates the expansion of B-cell progenitors in a dose-dependent manner. J. Biol. Chem. 288, 33449–33461. [PubMed: 24078629]

Anders S, Pyl PT, and Huber W (2015). HTSeq–a Python framework to work with high-throughput sequencing data. Bioinformatics 31, 166–169. [PubMed: 25260700]

Bereshchenko O, Lo Re O, Nikulenkov F, Flamini S, Kotaskova J, Mazza T, Le Pannérer MM, Buschbeck M, Giallongo C, Palumbo G, et al. (2019). Deficiency and haploinsufficiency of histone

macroH2A1.1 in mice recapitulate hematopoietic defects of human myelodysplastic syndrome. Clin. Epigenetics 11, 121. [PubMed: 31439048]

Boulard M, Storck S, Cong R, Pinto R, Delage H, and Bouvet P (2010). Histone variant macroH2A1 deletion in mice causes female-specific steatosis. Epigenetics Chromatin 3, 8. [PubMed: 20359320]

Bredemeyer AL, Sharma GG, Huang CY, Helmink BA, Walker LM, Khor KC, Nuskey B, Sullivan KE, Pandita TK, Bassing CH, and Sleckman BP (2006). ATM stabilizes DNA double-strand-break complexes during V(D)J recombination. Nature 442, 466–470. [PubMed: 16799570]

Buschbeck M, Uribesalgo I, Wibowo I, Rué P, Martin D, Gutierrez A, Morey L, Guigó R, López-Schier H, and Di Croce L (2009). The histone variant macroH2A is an epigenetic regulator of key developmental genes. Nat. Struct. Mol. Biol. 16, 1074–1079. [PubMed: 19734898]

Changolkar LN, and Pehrson JR (2006). macroH2A1 histone variants are depleted on active genes but concentrated on the inactive X chromosome. Mol. Cell. Biol. 26, 4410–4420. [PubMed: 16738309]

Chadwick BP, and Willard HF (2001). Histone H2A variants and the inactive X chromosome: identification of a second macroH2A variant. Hum. Mol. Genet. 10, 1101–1113. [PubMed: 11331621]

Changolkar LN, Costanzi C, Leu NA, Chen D, McLaughlin KJ, and Pehrson JR (2007). Developmental changes in histone macroH2A1-mediated gene regulation. Mol. Cell. Biol. 27, 2758–2764. [PubMed: 17242180]

Changolkar LN, Singh G, Cui K, Berletch JB, Zhao K, Disteche CM, and Pehrson JR (2010). Genome-wide distribution of macroH2A1 histone variants in mouse liver chromatin. Mol. Cell. Biol. 30, 5473–5483. [PubMed: 20937776]

Chen H, Ruiz PD, Novikov L, Casill AD, Park JW, and Gamble MJ (2014). MacroH2A1.1 and PARP-1 cooperate to regulate transcription by promoting CBP-mediated H2B acetylation. Nat. Struct. Mol. Biol. 21, 981–989. [PubMed: 25306110]

Chen L, Chen JY, Huang YJ, Gu Y, Qiu J, Qian H, Shao C, Zhang X, Hu J, Li H, et al. (2018). The Augmented R-Loop Is a Unifying Mechanism for Myelodysplastic Syndromes Induced by High-Risk Splicing Factor Mutations. Mol. Cell 69, 412–425.e6. [PubMed: 29395063]

Costanzi C, and Pehrson JR (1998). Histone macroH2A1 is concentrated in the inactive X chromosome of female mammals. Nature 393, 599–601. [PubMed: 9634239]

Coulon A, Ferguson ML, de Turris V, Palangat M, Chow CC, and Larson DR (2014). Kinetic competition during the transcription cycle results in stochastic RNA processing. eLife 3, e03939.

Damm F, Kosmider O, Gelsi-Boyer V, Renneville A, Carbuccia N, Hidalgo-Curtis C, Della Valle V, Couronné L, Scourzic L, Chesnais V, et al.; Groupe Francophone des Myélodysplasies (2012). Mutations affecting mRNA splicing define distinct clinical phenotypes and correlate with patient outcome in myelodysplastic syndromes. Blood 119, 3211–3218. [PubMed: 22343920]

Dardenne E, Pierredon S, Driouch K, Gratadou L, Lacroix-Triki M, Espinoza MP, Zonta E, Germann S, Mortada H, Villemin JP, et al. (2012). Splicing switch of an epigenetic regulator by RNA helicases promotes tumor-cell invasiveness. Nat. Struct. Mol. Biol. 19, 1139–1146. [PubMed: 23022728]

Dell'Orso S, Wang AH, Shih HY, Saso K, Berghella L, Gutierrez-Cruz G, Ladurner AG, O'Shea JJ, Sartorelli V, and Zare H (2016). The Histone Variant MacroH2A1.2 Is Necessary for the Activation of Muscle Enhancers and Recruitment of the Transcription Factor Pbx1. Cell Rep. 14, 1156–1168. [PubMed: 26832413]

Dobin A, Davis CA, Schlesinger F, Drenkow J, Zaleski C, Jha S, Batut P, Chaisson M, and Gingeras TR (2013). STAR: ultrafast universal RNA-seq aligner. Bioinformatics 29, 15–21. [PubMed: 23104886]

Fei DL, Zhen T, Durham B, Ferrarone J, Zhang T, Garrett L, Yoshimi A, Abdel-Wahab O, Bradley RK, Liu P, and Varmus H (2018). Impaired hematopoiesis and leukemia development in mice with a conditional knock-in allele of a mutant splicing factor gene *U2af1*. Proc. Natl. Acad. Sci. USA 115, E10437–E10446. [PubMed: 30322915]

Gamble MJ, Frizzell KM, Yang C, Krishnakumar R, and Kraus WL (2010). The histone variant macroH2A1 marks repressed autosomal chromatin, but protects a subset of its target genes from silencing. Genes Dev. 24, 21–32. [PubMed: 20008927]

Graubert TA, Shen D, Ding L, Okeyo-Owuor T, Lunn CL, Shao J, Krysiak K, Harris CC, Koboldt DC, Larson DE, et al. (2011). Recurrent mutations in the U2AF1 splicing factor in myelodysplastic syndromes. Nat. Genet. 44, 53–57. [PubMed: 22158538]

Hardy RR, Carmack CE, Shinton SA, Kemp JD, and Hayakawa K (1991). Resolution and characterization of pro-B and pre-pro-B cell stages in normal mouse bone marrow. J. Exp. Med. 173, 1213–1225. [PubMed: 1827140]

Heng TS, and Painter MW; Immunological Genome Project Consortium (2008). The Immunological Genome Project: networks of gene expression in immune cells. Nat. Immunol. 9, 1091–1094. [PubMed: 18800157]

Hodge DQ, Cui J, Gamble MJ, and Guo W (2018). Histone Variant MacroH2A1 Plays an Isoform-Specific Role in Suppressing Epithelial-Mesenchymal Transition. Sci. Rep. 8, 841. [PubMed: 29339820]

Hu Y, and Smyth GK (2009). ELDA: extreme limiting dilution analysis for comparing depleted and enriched populations in stem cell and other assays. J. Immunol. Methods 347, 70–78. [PubMed: 19567251]

Ilagan JO, Ramakrishnan A, Hayes B, Murphy ME, Zebari AS, Bradley P, and Bradley RK (2015). U2AF1 mutations alter splice site recognition in hematological malignancies. Genome Res. 25, 14–26. [PubMed: 25267526]

Jensen CT, Åhsberg J, Sommarin MNE, Strid T, Somasundaram R, Okuyama K, Ungerbäck J, Kupari J, Airaksinen MS, Lang S, et al. (2018). Dissection of progenitor compartments resolves developmental trajectories in B-lymphopoiesis. J. Exp. Med. 215, 1947–1963. [PubMed: 29899037]

Jiang XX, Nguyen Q, Chou Y, Wang T, Nandakumar V, Yates P, Jones L, Wang L, Won H, Lee HR, et al. (2011). Control of B cell development by the histone H2A deubiquitinase MYSM1. Immunity 35, 883–896. [PubMed: 22169041]

Kim D, Langmead B, and Salzberg SL (2015a). HISAT: a fast spliced aligner with low memory requirements. Nat. Methods 12, 357–360. [PubMed: 25751142]

Kim E, Ilagan JO, Liang Y, Daubner GM, Lee SC, Ramakrishnan A, Li Y, Chung YR, Micol JB, Murphy ME, et al. (2015b). SRSF2 Mutations Contribute to Myelodysplasia by Mutant-Specific Effects on Exon Recognition. Cancer Cell 27, 617–630. [PubMed: 25965569]

Koboldt D, Zhang Q, Larson D, Shen D, McLellan M, Lin L, Miller C, Mardis E, Ding L, and Wilson R (2012). VarScan 2: Somatic mutation and copy number alteration discovery in cancer by exome sequencing. Genome Res. 22, 568–576. [PubMed: 22300766]

Kon A, Yamazaki S, Nannya Y, Kataoka K, Ota Y, Nakagawa MM, Yoshida K, Shiozawa Y, Morita M, Yoshizato T, et al. (2018). Physiological *Srsf2* P95H expression causes impaired hematopoietic stem cell functions and aberrant RNA splicing in mice. Blood 131, 621–635. [PubMed: 29146882]

Law CW, Chen Y, Shi W, and Smyth GK (2014). voom: Precision weights unlock linear model analysis tools for RNA-seq read counts. Genome Biol. 15, R29. [PubMed: 24485249]

Ley TJ, Miller C, Ding L, Raphael BJ, Mungall AJ, Robertson A, Hoadley K, Triche TJ Jr., Laird PW, Baty JD, et al.; Cancer Genome Atlas Research Network (2013). Genomic and epigenomic landscapes of adult de novo acute myeloid leukemia. N. Engl. J. Med. 368, 2059–2074. [PubMed: 23634996]

Li F, Yi P, Pi J, Li L, Hui J, Wang F, Liang A, and Yu J (2016). QKI5-mediated alternative splicing of the histone variant macroH2A1 regulates gastric carcinogenesis. Oncotarget 7, 32821–32834. [PubMed: 27092877]

Liu T, Ahmed T, Krysiak K, Shirai CL, Shao J, Nunley R, Bucala R, McKenzie A, Ndonwi M, and Walter MJ (2020). Haploinsufficiency of multiple del(5q) genes induce B cell abnormalities in mice. Leuk. Res. 96, 106428. [PubMed: 32739655]

Love MI, Huber W, and Anders S (2014). Moderated estimation of fold change and dispersion for RNA-seq data with DESeq2. Genome Biol. 15, 550. [PubMed: 25516281]

Mainville CA, Parmar K, Unnikrishnan I, Gong L, Raffel GD, and Rosenberg N (2001). Temperature-sensitive transformation by an Abelson virus mutant encoding an altered SH2 domain. J. Virol. 75, 1816–1823. [PubMed: 11160680]

Mortera-Blanco T, Dimitriou M, Woll PS, Karimi M, Elvarsdottir E, Conte S, Tobiasson M, Jansson M, Douagi I, Moarii M, et al. (2017). *SF3B1*-initiating mutations in MDS-RSs target lymphomyeloid hematopoietic stem cells. Blood 130, 881–890. [PubMed: 28634182]

Mupo A, Seiler M, Sathiaseelan V, Pance A, Yang Y, Agrawal AA, Iorio F, Bautista R, Pacharne S, Tzelepis K, et al. (2017). Hemopoietic-specific Sf3b1-K700E knock-in mice display the splicing defect seen in human MDS but develop anemia without ring sideroblasts. Leukemia 31, 720–727. [PubMed: 27604819]

Nguyen HD, Yadav T, Giri S, Saez B, Graubert TA, and Zou L (2017). Functions of Replication Protein A as a Sensor of R Loops and a Regulator of RNaseH1. Mol. Cell 65, 832–847.e4. [PubMed: 28257700]

Nguyen HD, Leong WY, Li W, Reddy PNG, Sullivan JD, Walter MJ, Zou L, and Graubert TA (2018). Spliceosome Mutations Induce R Loop-Associated Sensitivity to ATR Inhibition in Myelodysplastic Syndromes. Cancer Res. 78, 5363–5374. [PubMed: 30054334]

Novikov L, Park JW, Chen H, Klerman H, Jalloh AS, and Gamble MJ (2011). QKI-mediated alternative splicing of the histone variant MacroH2A1 regulates cancer cell proliferation. Mol. Cell. Biol. 31, 4244–4255. [PubMed: 21844227]

Obeng EA, Chappell RJ, Seiler M, Chen MC, Campagna DR, Schmidt PJ, Schneider RK, Lord AM, Wang L, Gambe RG, et al. (2016). Physiologic Expression of Sf3b1(K700E) Causes Impaired Erythropoiesis, Aberrant Splicing, and Sensitivity to Therapeutic Spliceosome Modulation. Cancer Cell 30, 404–417. [PubMed: 27622333]

Ogata K, Kishikawa Y, Satoh C, Tamura H, Dan K, and Hayashi A (2006). Diagnostic application of flow cytometric characteristics of CD34+ cells in low-grade myelodysplastic syndromes. Blood 108, 1037–1044. [PubMed: 16574954]

Okeyo-Owuor T, White BS, Chatrikhi R, Mohan DR, Kim S, Griffith M, Ding L, Ketkar-Kulkarni S, Hundal J, Laird KM, et al. (2015). U2AF1 mutations alter sequence specificity of pre-mRNA binding and splicing. Leukemia 29, 909–917. [PubMed: 25311244]

Papaemmanuil E, Cazzola M, Boultwood J, Malcovati L, Vyas P, Bowen D, Pellagatti A, Wainscoat JS, Hellstrom-Lindberg E, Gambacorti-Passerini C, et al.; Chronic Myeloid Disorders Working Group of the International Cancer Genome Consortium (2011). Somatic SF3B1 mutation in myelodysplasia with ring sideroblasts. N. Engl. J. Med. 365, 1384–1395. [PubMed: 21995386]

Park SM, Ou J, Chamberlain L, Simone TM, Yang H, Virbasius CM, Ali AM, Zhu LJ, Mukherjee S, Raza A, and Green MR (2016). U2AF35(S34F) Promotes Transformation by Directing Aberrant ATG7 Pre-mRNA 3′ End Formation. Mol. Cell 62, 479–490. [PubMed: 27184077]

Pehrson JR, Costanzi C, and Dharia C (1997). Developmental and tissue expression patterns of histone macroH2A1 subtypes. J. Cell. Biochem. 65, 107–113. [PubMed: 9138085]

Pehrson JR, Changolkar LN, Costanzi C, and Leu NA (2014). Mice without macroH2A histone variants. Mol. Cell. Biol. 34, 4523–4533. [PubMed: 25312643]

Pertea M, Pertea GM, Antonescu CM, Chang TC, Mendell JT, and Salzberg SL (2015). StringTie enables improved reconstruction of a transcriptome from RNA-seq reads. Nat. Biotechnol. 33, 290–295. [PubMed: 25690850]

Posavec Marjanović M, Hurtado-Bagès S, Lassi M, Valero V, Malinverni R, Delage H, Navarro M, Corujo D, Guberovic I, Douet J, et al. (2017). MacroH2A1.1 regulates mitochondrial respiration by limiting nuclear NAD^+ consumption. Nat. Struct. Mol. Biol. 24, 902–910. [PubMed: 28991266]

Reis-Alves SC, Traina F, Metze K, and Lorand-Metze I (2015). Improving the differential diagnosis between myelodysplastic syndromes and reactive peripheral cytopenias by multiparametric flow cytometry: the role of B-cell precursors. Diagn. Pathol. 10, 44. [PubMed: 25924846]

Robinson MD, McCarthy DJ, and Smyth GK (2010). edgeR: a Bioconductor package for differential expression analysis of digital gene expression data. Bioinformatics 26, 139–140. [PubMed: 19910308]

Shirai CL, Ley JN, White BS, Kim S, Tibbitts J, Shao J, Ndonwi M, Wadugu B, Duncavage EJ, Okeyo-Owuor T, et al. (2015). Mutant U2AF1 Expression Alters Hematopoiesis and Pre-mRNA Splicing In Vivo. Cancer Cell 27, 631–643. [PubMed: 25965570]

Singh S, Ahmed D, Dolatshad H, Tatwavedi D, Schulze U, Sanchi A, Ryley S, Dhir A, Carpenter L, Watt SM, et al. (2020). SF3B1 mutations induce R-loop accumulation and DNA damage in MDS and leukemia cells with therapeutic implications. Leukemia 34, 2525–2530. [PubMed: 32076118]

Smeets MF, Tan SY, Xu JJ, Anande G, Unnikrishnan A, Chalk AM, Taylor SR, Pimanda JE, Wall M, Purton LE, and Walkley CR (2018). *Srsf2*^{P95H} initiates myeloid bias and myelodysplastic/myeloproliferative syndrome from hemopoietic stem cells. Blood 132, 608–621. [PubMed: 29903888]

Soodgupta D, White LS, Yang W, Johnston R, Andrews JM, Kohyama M, Murphy KM, Mosammaparast N, Payton JE, and Bednarski JJ (2019). RAG-Mediated DNA Breaks Attenuate PU.1 Activity in Early B Cells through Activation of a SPIC-BCLAF1 Complex. Cell Rep. 29, 829–843.e5. [PubMed: 31644907]

Sporn JC, and Jung B (2012). Differential regulation and predictive potential of MacroH2A1 isoforms in colon cancer. Am. J. Pathol. 180, 2516–2526. [PubMed: 22542848]

Sporn JC, Kustatscher G, Hothorn T, Collado M, Serrano M, Muley T, Schnabel P, and Ladurner AG (2009). Histone macroH2A isoforms predict the risk of lung cancer recurrence. Oncogene 28, 3423–3428. [PubMed: 19648962]

Sternberg A, Killick S, Littlewood T, Hatton C, Peniket A, Seidl T, Soneji S, Leach J, Bowen D, Chapman C, et al. (2005). Evidence for reduced B-cell progenitors in early (low-risk) myelodysplastic syndrome. Blood 106, 2982–2991. [PubMed: 16076868]

Sun Z, and Bernstein E (2019). Histone variant macroH2A: from chromatin deposition to molecular function. Essays Biochem. 63, 59–74. [PubMed: 31015383]

Sun Z, Filipescu D, Andrade J, Gaspar-Maia A, Ueberheide B, and Bernstein E (2018). Transcription-associated histone pruning demarcates macroH2A chromatin domains. Nat. Struct. Mol. Biol. 25, 958–970. [PubMed: 30291361]

Thol F, Kade S, Schlarmann C, Löffeld P, Morgan M, Krauter J, Wlodarski MW, Kölking B, Wichmann M, Görlich K, et al. (2012). Frequency and prognostic impact of mutations in SRSF2, U2AF1, and ZRSR2 in patients with myelodysplastic syndromes. Blood 119, 3578–3584. [PubMed: 22389253]

Visconte V, Makishima H, Jankowska A, Szpurka H, Traina F, Jerez A, O'Keefe C, Rogers HJ, Sekeres MA, Maciejewski JP, and Tiu RV (2012). SF3B1, a splicing factor is frequently mutated in refractory anemia with ring sideroblasts. Leukemia 26, 542–545. [PubMed: 21886174]

Yang Q, Shi M, Shen Y, Cao Y, Zuo S, Zuo C, Zhang H, Gabrilovich DI, Yu Y, and Zhou J (2014). COX-1–derived thromboxane A_2 plays an essential role in early B-cell development via regulation of JAK/STAT5 signaling in mouse. Blood 124, 1610–1621. [PubMed: 25030064]

Yip BH, Steeples V, Repapi E, Armstrong RN, Llorian M, Roy S, Shaw J, Dolatshad H, Taylor S, Verma A, et al. (2017). The U2AF1S34F mutation induces lineage-specific splicing alterations in myelodysplastic syndromes. J. Clin. Invest. 127, 3557.

Yoshida K, Sanada M, Shiraishi Y, Nowak D, Nagata Y, Yamamoto R, Sato Y, Sato-Otsubo A, Kon A, Nagasaki M, et al. (2011). Frequent pathway mutations of splicing machinery in myelodysplasia. Nature 478, 64–69. [PubMed: 21909114]

Yu G, Wang LG, Han Y, and He QY (2012). clusterProfiler: an R package for comparing biological themes among gene clusters. OMICS 16, 284–287. [PubMed: 22455463]

Highlights

- Mutant U2AF1(S34F) induces alternative splicing of *H2AFY*
- *H2afy*$^{-/-}$ mice have defective B cell development similar to U2AF1(S34F) mice
- The *H2afy1.1* splice isoform, reduced by U2AF1(S34F), regulates B cell development
- H2AFY occupies the *Ebf1* promoter, a master regulator of B cell development

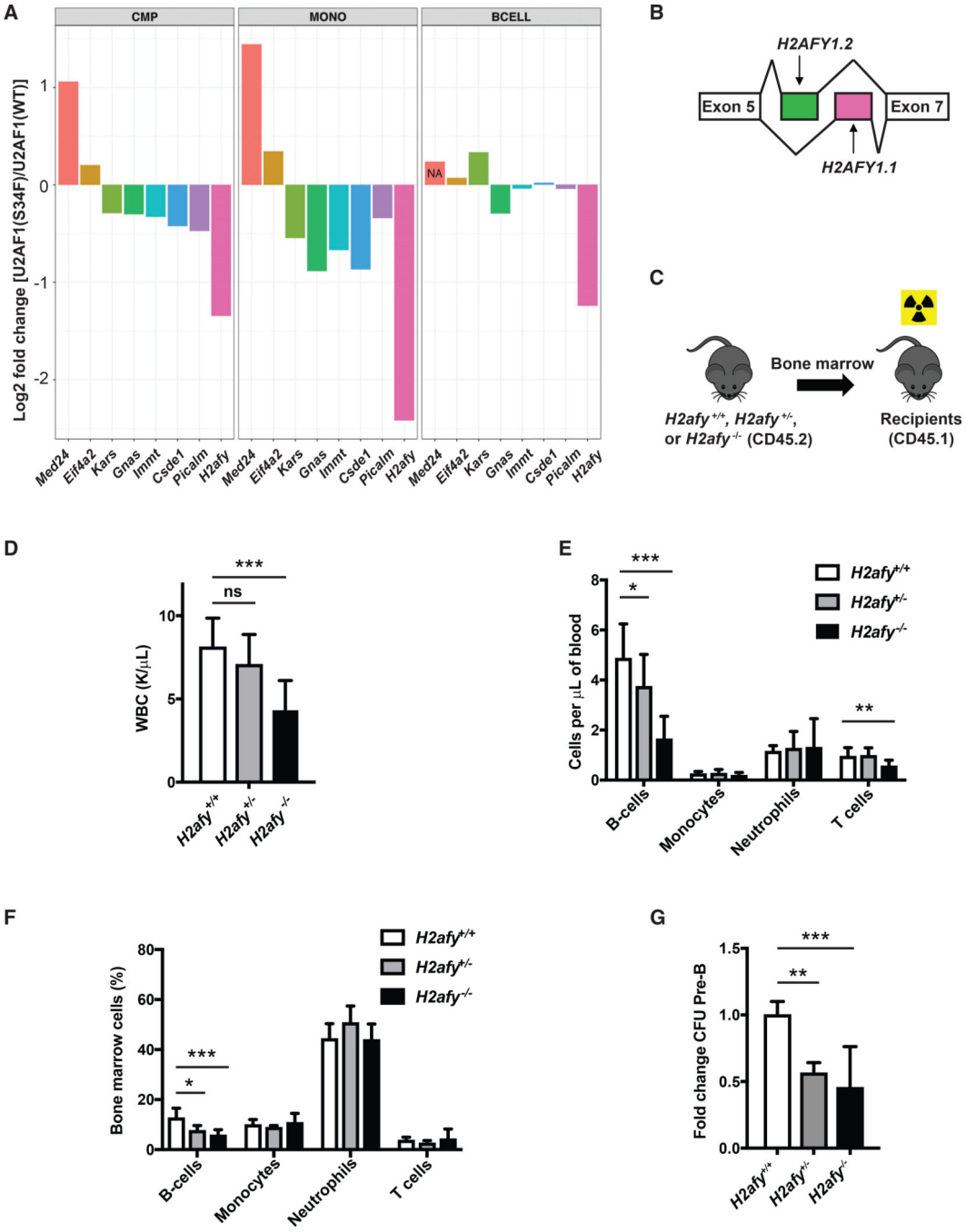

Figure 1. *H2afy* is a target gene of U2AF1(S34F)-induced alternative splicing

(A) Expression of U2AF1(S34)-induced alternatively spliced isoforms in eight genes in common myeloid progenitors (CMPs), monocytes (MONO) and B cells in mice were examined using a Nanostring assay. Log2-fold change of U2AF1(S34F) samples compared to U2AF1(WT) samples are shown (n = 2–9 biologic replicates per tissue).

(B) Diagram showing two *H2AFY* splice isoforms, *H2AFY1.1* and *H2AFY1.2*.

(C–G) Whole bone marrow cells from *H2afy*$^{+/+}$, *H2afy*$^{+/-}$ and *H2afy*$^{-/-}$ littermates were transplanted into lethally irradiated WT congenic recipient mice. (C) Overview of the non-

competitive bone marrow transplant assay. (D) Peripheral blood WBCs at 4 months post-transplant (n = 13–17). (E) Peripheral blood lineage cell counts at 4 months post-transplant (n = 13–17). (F) Bone marrow lineage cell frequencies at 12 months post-transplant (n = 5–15). (G) Pre-B cell colonies in the CFU-pre-B assay (n = 10–16).

Data are shown as fold change of colonies of *H2afy*$^{+/-}$ or *H2afy*$^{-/-}$ pre-B cells relative to *H2afy*$^{+/+}$ colonies. Statistical analysis by two-tailed Student's t test. Error bars represent mean ± SD. ns, not significant; *p < 0.05, **p < 0.01, ***p < 0.001.

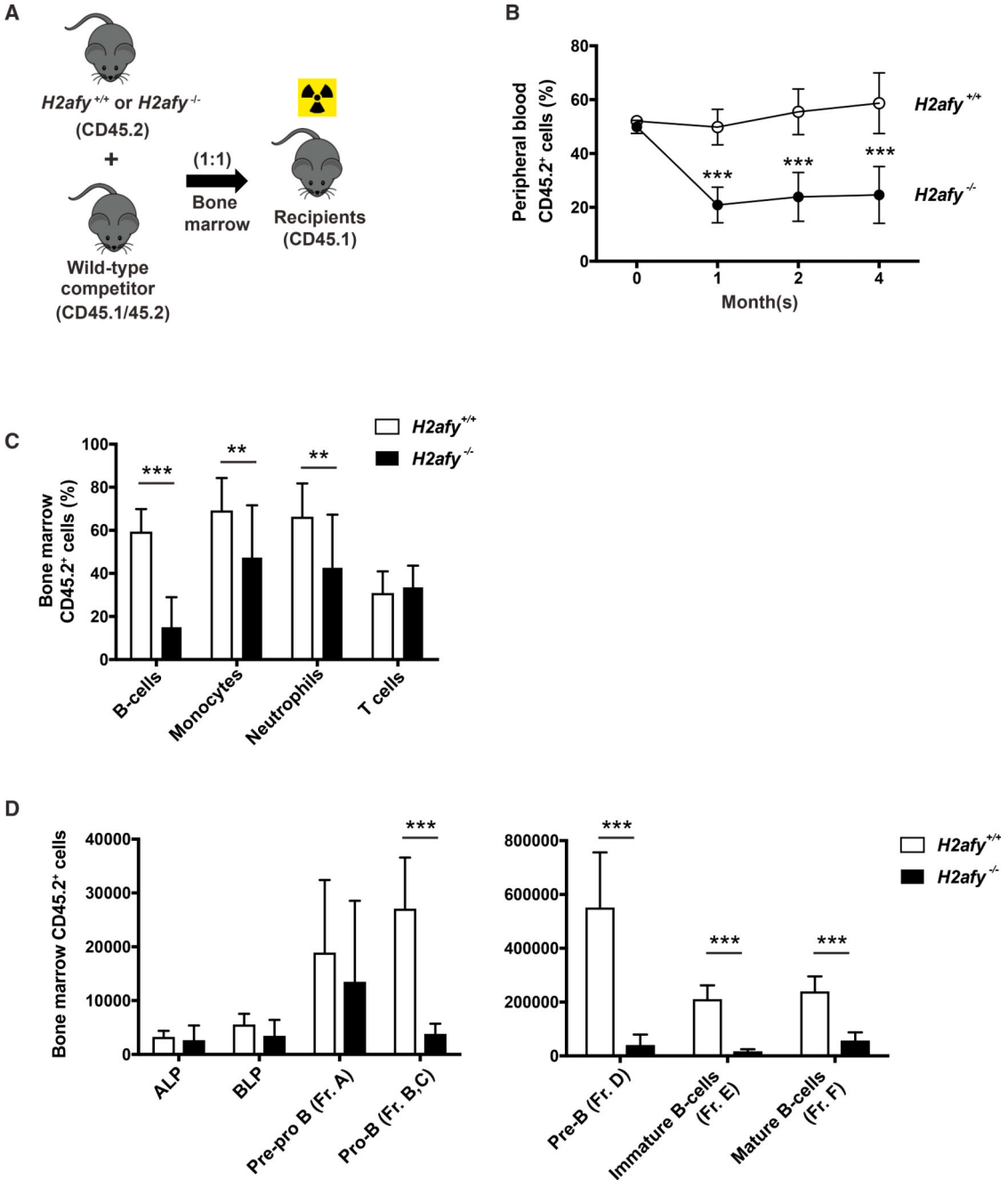

Figure 2. *H2afy*$^{-/-}$ mice have defective B cell development

A competitive repopulation assay was performed by transplanting bone marrow cells from *H2afy*$^{+/+}$ or *H2afy*$^{-/-}$ littermates (CD45.2^{+}) with the same number of WT congenic competitor marrow cells (CD45.1^{+}/CD45.2^{+}) into lethally irradiated congenic recipients (CD45.1^{+}).

(A) Overview of the competitive repopulation assay.

(B) Peripheral blood chimerism of CD45.2^{+} cells at 1, 2, and 4 month(s) post-transplant (n = 16). Differences (two-way ANOVA) are indicated at each time point.

(C) CD45.2^{+} bone marrow lineage cell frequencies at 4 months post-transplant (n = 7).

(D) Donor-derived CD45.2^{+} B cell progenitors (ALP and BLP) and Hardy fractions (n = 7). Statistical analysis by two-tailed Student's t test, except for (B). Error bars represent mean ± SD. ns, not significant; *p < 0.05, **p < 0.01, ***p < 0.001.

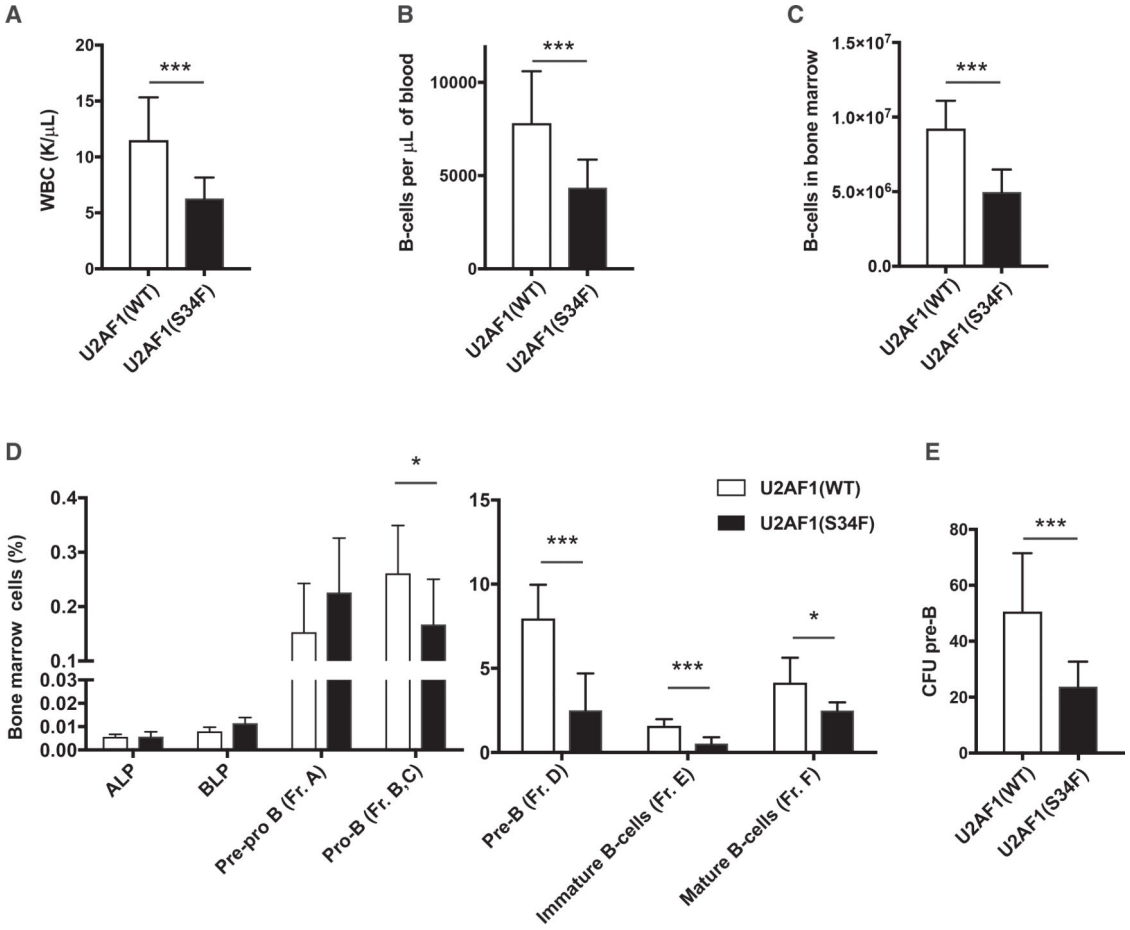

Figure 3. U2AF1(S34F) expression induces defective B cell development

Analysis of recipient mice transplanted with bone marrow cells from transgenic U2AF1(WT) or U2AF1(S34F) mice following 1 month of doxycycline induction (n = 10).

(A) Peripheral blood WBC count.

(B) Peripheral blood B cell counts.

(C) Bone marrow B cell counts.

(D) Frequencies of B cell progenitors (ALP and BLP) and Hardy fractions.

(E) The number of pre-B cell colonies in the CFU-pre-B assay.

Statistical analysis by two-tailed Student's t test. Error bars represent mean ± SD. ns, not significant; *p < 0.05, **p < 0.01, ***p < 0.001.

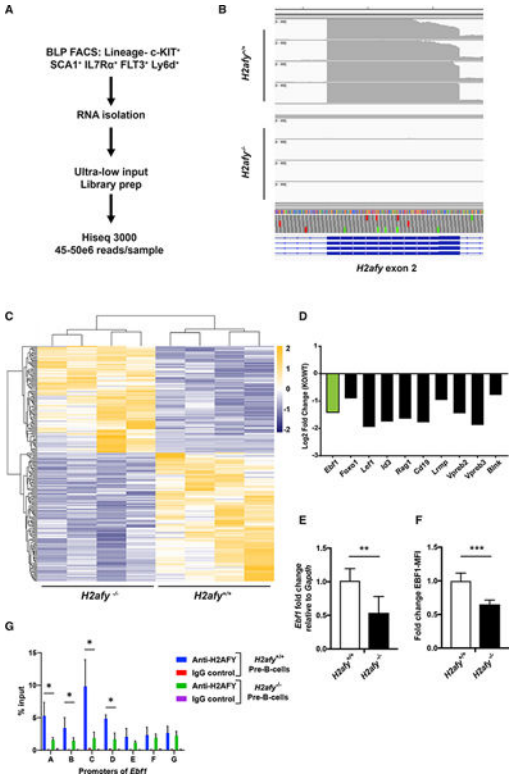

Figure 4. *Ebf1* expression is reduced in *H2afy*$^{-/-}$ BLPs

(A) Schematic of BLP RNA-seq (n = 4).

(B) Read counts against exon 2 of *H2afy*.

(C) Heatmap showing 214 DEGs (FDR < 0.1).

(D) *Ebf1* and its target gene expression in the BLP RNA-seq data. Log2-fold change of *Ebf1* and its target gene RNA expression from RNA-seq data is shown.

(E) Changes in *Ebf1* expression upon *H2afy* loss. A fold change of RNA expression of *Ebf1* relative to *Gapdh* in sorted BLPs was determined by qRT-PCR (n = 5).

(F) EBF1 protein expression by intracellular flow cytometry. A fold change of mean fluorescence intensity (MFI) is indicated (n = 5).

(G) Enrichment of H2AFY at the promoter of *Ebf1* in WT (*H2afy*$^{+/+}$) and *H2afy*$^{-/-}$ pre-B cell lines measured by chromatin immunoprecipitation followed by qPCR (n = 4).

Statistical analysis by two-tailed Student's t test. Error bars represent mean ± SD. *p < 0.05, **p < 0.01, ***p < 0.001.

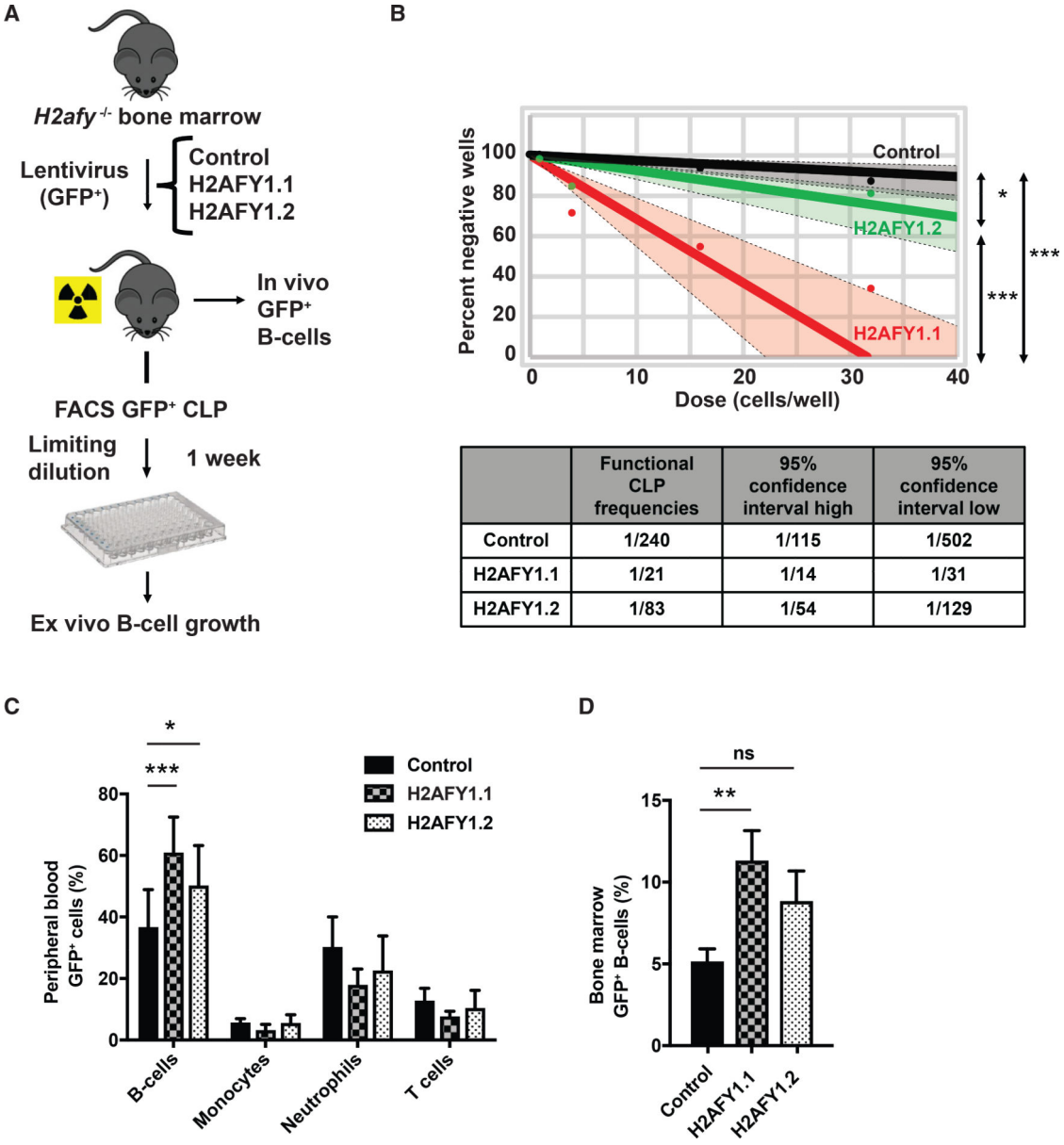

	Functional CLP frequencies	95% confidence interval high	95% confidence interval low
Control	1/240	1/115	1/502
H2AFY1.1	1/21	1/14	1/31
H2AFY1.2	1/83	1/54	1/129

Figure 5. Expression of *H2AFY1.1* in *H2afy*$^{-/-}$ bone marrow cells rescues reduced B cells *ex vivo* and *in vivo*

H2afy$^{-/-}$ bone marrow cells were transduced with control lentivirus (GFP alone), *H2AFY1.1*-, or *H2AFY1.2*-expressing lentivirus that co-expressed GFP and transplanted into lethally irradiated congenic CD45.1^{+} recipients.

(A) Overview of the experimental design.

(B) Limiting dilution assay of functional CLPs (GFP^{+}). Top panel: percent negative wells are plotted against the number of cells seeded per well. Bottom table: quantification of frequencies of functional CLPs with 95% confidence intervals. Data were pooled from four independent experiments, each consisting of 12–24 replicates.

(C) Peripheral blood GFP^{+} lineage cells at 4 months post-transplant (n = 8–10).

(D) Bone marrow GFP^{+} B cells at 4 months post-transplant (n = 5–7).

Statistical analysis by two-tailed Student's t test, except for (B). Error bars represent mean ± SD. ns, not significant; *p < 0.05, **p < 0.01, ***p < 0.001.

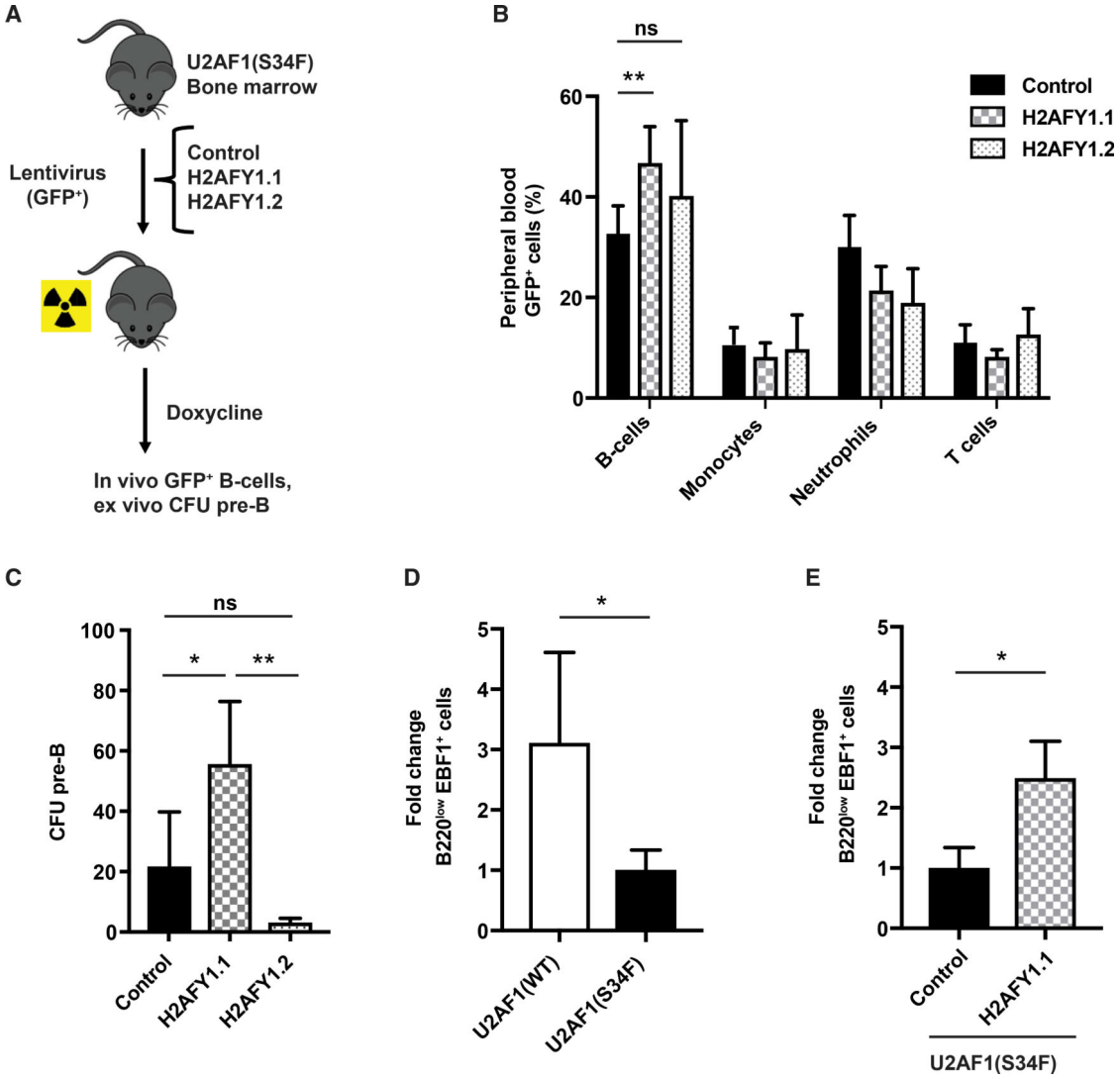

Figure 6. Expression of *H2AFY1.1* in U2AF1(S34F) bone marrow cells rescues reduced B cells *ex vivo* and *in vivo*

In (A)–(C) and (E), bone marrow cells from transgenic U2AF1(S34F) mice were transduced with control lentivirus (GFP alone), *H2AFY1.1*-, or *H2AFY1.2*-expressing lentivirus that co-expressed GFP and transplanted into lethally irradiated congenic CD45.1^{+} recipients. Recipient mice were treated with doxycycline for 6 months.

(A) Overview of the experimental design.

(B) Peripheral blood GFP^{+} lineage cells after 6 months of transgene induction with doxycycline (n = 7–10).

(C) CFU-pre-B counts of sorted GFP^{+} bone marrow cells (n = 5).

(D) Following 1 month of doxycycline induction, B220^{low}EBF1^{+} cells in the bone marrow of U2AF1(WT) and U2AF1(S34F) mice were measured by flow cytometry (n = 4–5). Data are shown as fold change of the U2AF1(WT) samples relative to the U2AF1(S34F) samples.

(E) GFP^{+}B220^{low}EBF1^{+} cells were measured by flow cytometry after 6 months of transgene induction (n = 3).

Data are shown as fold change of *H2AFY1.1*-expressing samples relative to control samples (GFP^+). Statistical analysis by two-tailed Student's t test. Error bars represent mean ± SD. ns, not significant; *p < 0.05, **p < 0.01, ***p < 0.001.